AJRCCM Articles in Press. Published on 25-July-2018 as 10.1164/rccm.201708-1580OC

Increased extracellular vesicles mediate WNT-5A signaling in idiopathic pulmonary fibrosis

Aina Martin-Medina[1], Mareike Lehmann[1], Olivier Burgy[2], Sarah Hermann[1], Hoeke A. Baarsma[1], Darcy E. Wagner[1], Martina M. De Santis[1], Florian Ciolek[1], Thomas P. Hofer[1,3], Marion Frankenberger[1], Michaela Aichler[4], Michael Lindner[3], Wolfgang Gesierich[3], Andreas Guenther[5,6,7], Axel Walch[4], Christina Coughlan[8], Paul Wolters[9], Joyce S. Lee[2], Jürgen Behr[1,3], Melanie Königshoff[1,2]

[1]Comprehensive Pneumology Center, Ludwig Maximilian University, University Hospital Grosshadern, and Helmholtz Zentrum München, Munich, Germany; Member of the German Center of Lung Research (DZL); [2]Division of Pulmonary Sciences and Critical Care Medicine, Department of Medicine, University of Colorado Denver, Aurora, CO, USA; [3] Center for Thoracic Surgery, Asklepios Biobank for Lung Diseases, Asklepios Clinic Munich-Gauting, Munich, Germany; [4]Institute of Pathology, Research Unit Analytical Pathology, Helmholtz Zentrum München, Germany ; [5]Dept of Internal Medicine, Universities of Giessen and Marburg Lung Center (UGMLC), Justus-Liebig-Universität Giessen, Member of the German Center for Lung Research (DZL), Giessen, Germany; [6]Agaplesion Lung Clinic Waldhof Elgershausen, Greifenstein, Germany; [7]European IPF Network and European IPF Registry; [8] Department of Neurology, University of Colorado Denver, Aurora, CO, USA; [9]Division of Pulmonary and Critical Care Medicine, Department of Medicine, University of California, San Francisco, CA.

Corresponding author: melanie.koenigshoff@ucdenver.edu

Division of Pulmonary Sciences and Critical Care Medicine, Department of Medicine, University of Colorado – Denver, AMC, Research 2, 9th Flr, 12700 East 19th Ave, Aurora, CO 80045

Author contributions

A.M.-M., O.B., S.H., D.S.M. and F.C. designed and performed experiments and data analysis; M.L. and M.K. designed experiments and oversaw all data analysis; D.E.W. performed histograms and data analysis in Fig. 1.; T. P. H., M.F., M. Lindner, A.G. and J.B. collected and provided human BALF and tissue samples; C.G. contributed to nanoparticles tracking experiments and analysis; J.S.L. and P.W. provided human BALF samples; M. A. and A.W. performed electron transmission microscopy; A.M.-M., M.L, O.B., H.A.B. and M.K. drafted the manuscript; All authors have critically revised the manuscript. All authors have read, reviewed and approved the final manuscript as submitted to take public responsibility for it.

Funding

This work was funded by a W2/W3 Professorship Award to M.K. from the Helmholtz Association, Germany. O.B. is supported by a postdoctoral fellowship from the European Respiratory Society and the European Molecular Biology Organization (ERS/EMBO Joint Research Fellowship – Nr. LTRF 2016 – 7481). H.A.B. is supported by the Helmholtz Munich Postdoctoral Program. D.E.W. is supported by a Whitaker International Scholar Fellowship and the Helmholtz Munich Postdoctoral Program. The UCSF cohort is supported by the Nina Ireland Program for Lung Health.

AJRCCM Articles in Press. Published on 25-July-2018 as 10.1164/rccm.201708-1580OC

Competing financial interests: The authors declare no competing financial interests.

Running head: Increased extracellular vesicles contribute to IPF

Subject category list: 3.11 Pulmonary Fibrosis/Fibroblast Biology

Total word count body of the manuscript: 3500

This article has an online data supplement, which is accessible from this issue's table of content online at www.atsjournals.org

At a glance commentary:

Scientific knowledge on the subject: Extracellular vesicles (EVs) are potent mediators of intercellular communication and have recently been implicated in chronic lung diseases. However, the relevance of EVs in pulmonary fibrosis and their potential contribution to pathogenesis remains unexplored.

What this study adds to the field: We report for the first time that EVs are increased in experimental and human pulmonary fibrosis and lead to altered fibroblast function in disease. We show that the WNT protein WNT-5A is secreted on EVs and can be found in BALF from IPF patients. WNT-5A on EVs isolated from IPF BALF led to increased fibroblast proliferation, thus highlighting a pathophysiological role of EVs in IPF.

Abstract

Rationale: Idiopathic pulmonary fibrosis (IPF) is a lethal lung disease characterized by lung epithelial cell injury, increased (myo)fibroblast activation and extracellular matrix deposition. Extracellular vesicles (EVs) regulate intercellular communication by carrying a variety of signaling mediators, including WNT proteins. The relevance of EVs in pulmonary fibrosis and their potential contribution to disease pathogenesis, however, remains unexplored. **Objective:** To characterize EVs and study the role of EV-bound WNT signaling in IPF. **Methods:** We isolated EVs from bronchoalveolar lavage fluid (BALF) from experimental lung fibrosis as well as samples from IPF, non IPF-ILD, non-ILD and healthy volunteers from two independent cohorts. EVs were characterized by transmission electron microscopy, nanoparticle tracking analysis and Western Blotting (WB). Primary human lung fibroblasts (phLFs) were used for EV isolation and analyzed by metabolic activity assays, cell counting, qPCR and WB upon WNT gain- and loss-of-function studies. **Measurements and Main Results:** We found increased EVs, particularly exosomes, in BALF from experimental lung fibrosis as well as from IPF patients. WNT-5A was secreted on EVs in lung fibrosis and induced by TGF-β in primary human lung fibroblasts. The phLF-derived EVs induced phLF proliferation, which was attenuated by WNT-5A silencing and antibody-mediated inhibition and required intact EV structure. Similarly, EVs from IPF-BALF induced phLF proliferation, which was mediated by WNT-5A. **Conclusions:** Increased EVs function as carriers for signaling mediators, such as WNT-5A, in IPF and thus contribute to disease pathogenesis. Characterization of EV secretion and composition may lead to novel approaches to diagnose and develop treatments for pulmonary fibrosis.

AJRCCM Articles in Press. Published on 25-July-2018 as 10.1164/rccm.201708-1580OC

Total word count: 250

Key words: lung fibrosis, exosomes, lung fibroblasts, proliferation, WNT-5A

Introduction

Idiopathic pulmonary fibrosis (IPF) is a lethal interstitial lung disease of yet unknown etiology and limited therapeutic options. Current evidence suggests that IPF is a result of ongoing lung epithelial cell injury and aberrant wound healing, which impairs epithelial to mesenchymal crosstalk and subsequently leads to myofibroblast activation and increased deposition of extracellular matrix components (1, 2). Extracellular vesicles (EVs) are membranous-like vesicles with a diameter between 30-2000 nm capable of transporting proteins, lipids and nucleic acids (3) and are mediators of intercellular communication under both physiological and disease conditions (4). Recent studies have highlighted the potential contribution of EVs to chronic lung diseases and have investigated the role of serum-derived EVs as potential biomarkers (5-7). The expression and function of EVs in the local lung environment in the context of lung fibrosis and remodeling, however, remains largely unexplored.

Alterations in the WNT signaling pathways are known to contribute to cellular (dys)functions in pulmonary fibrosis (8-10) and more recently, it has been demonstrated that secreted WNT proteins can be transported by EVs to exert their intercellular communication (11). The vast majority of research has focused on the role of the WNT/β-catenin pathway in pulmonary fibrosis, which has been linked to disturbed lung epithelial cell function and impaired repair (8-10, 12). β-catenin independent WNT signaling in lung fibrosis is much less studied. The WNT protein WNT-5A is largely known to exert its effects β-catenin independent and has been found upregulated in IPF fibroblasts (13). However, its potential involvement in EV-mediated signaling has not been investigated. In this study we aimed to characterize the EV secretion profile in

AJRCCM Articles in Press. Published on 25-July-2018 as 10.1164/rccm.201708-1580OC

both experimental and human pulmonary fibrosis, and to investigate the secretion of WNT proteins on EVs. We have characterized EVs in BALF from IPF compared to non-IPF-ILD/non-ILD patients as well as healthy volunteers in two independent cohorts. IPF-derived EVs carry WNT-5A and we identified lung fibroblasts as a major source of EV-bound WNT-5A. IPF-derived EVs drive fibroblast proliferation, which was largely dependent on WNT-5A. Thus, this study highlights EVs as potential mediators of disturbed cellular function and communication in IPF. Some of the results have been previously reported in the form of an abstract (14).

Material and Methods

Isolation and characterization of extracellular vesicles (EVs)

EVs were isolated from murine and human BALF samples, primary human cell cultures and mouse lung tissue using ultracentrifugation (Thermofisher Scientific, Sorvall, rotors: fixed-angle T635.5 and TFT80) following state-of-the-art protocols (15). For some EV isolations ExoQuick© (Systems Bioscience) was used as indicated in the manuscript text and figure legends. For all EV preparations, the EV-free-supernatant was stored at -80°C and the pellet containing EVs was re-suspended in 30-100 µl of sterile PBS and directly used or stored at -80°C. Characterization was performed using several methods as recommended in (15) and outlined in the supplemental material.

Detailed description of further material and methods is provided in the online data supplement.

Results

Extracellular vesicle (EV) secretion is upregulated in experimental and human lung fibrosis

First, we asked the question whether the amount of EV protein and EV number is altered in lung fibrosis. To this end, we isolated and characterized EVs from bronchoalveolar lavage fluid (BALF) from experimental and human lung fibrosis samples and controls (Fig. 1A). BALF was collected from mice 14 days after intratracheal bleomycin or PBS administration, or from IPF, non-IPF-ILD and non-ILD patients (Munich cohort, Table 1) as well as IPF patients and healthy volunteers (UCSF cohort, Table 2). Morphological assessment of EVs by transmission electron microscopy (TEM) revealed the presence of (i) large amounts of exosomes (smaller concave vesicles between 30 and 200nm, Fig. 1B and E1A; arrows), and (ii) a smaller fraction of microvesicles (irregular membranous vesicles between 200 and 1000nm, Fig. 1B and E1A; arrow heads). We further found enriched expression of the endosomal sorting complex required for transport component Tumor susceptibility gene 101 (TSG101), a protein commonly used to identify EVs (16) (Fig. E1B). TSG101 was increased in BALF-EVs from fibrotic lungs compared to BALF-EVs from control (Fig. E1B), suggesting a potential increase in EVs under fibrotic conditions. Moreover, we found a significantly increased amount of protein content in EVs from fibrotic compared to healthy mice (Fig. 1C, EV total µg protein/mL: PBS 51.3±25.32, Bleo 266.2±114.8, P=0.0001). Next, we quantified EV numbers and determined the size distribution by nanoparticle tracking analysis (NTA) (Fig. 1D) or by dynamic light scattering (Fig. E1C). By NTA, we found increased number of EVs in the BALF from fibrotic mouse lungs compared to controls, in particular exosomes, indicating a change in number and size distribution of EVs upon fibrosis

AJRCCM Articles in Press. Published on 25-July-2018 as 10.1164/rccm.201708-1580OC

development (Fig. 1D, exosome particles/ml: PBS $1.93x10^8$±$6x10^6$, Bleo $4.3x10^8$±$1.9x10^8$, P=0.049). We next aimed to translate these findings into the human disease. We explored whether EVs can be found in human BALF from non-ILD, non-IPF ILD and IPF patients (Table 1, Munich Cohort,) as well as from BALF from IPF patients and healthy volunteers (Table 2, UCSF cohort). EVs were characterized by TEM (Fig. 1E), TSG101 expression, and the absence of Calreticulin (an ER marker absent in EVs) (Fig. E1D). We observed a significant upregulation of EV protein content in BALF from IPF patients compared to non-ILD/non-IPF-ILD (Fig. 1F, EV total µg protein/mL: non-ILD/non-IPF-ILD (n=12/7) 251.6±166.6, IPF (n=16) 552.3±427.3, P=0.0212). Further, using NTA, we found a significant increase in EVs, mainly corresponding to exosomes, (Fig. 1G, left and middle panels) in BALF from IPF patients in comparison to non-ILD/non-IPF-ILD (Fig. 1G, right panel, particles/mL of initial sample: non-ILD (n=7) $2.2x10^8$±$1.8x10^8$, non-IPF-ILD (n=6) $3.3x10^8$±$2.5x10^8$, and IPF (n=4) $6.0x10^8$±$3.8x10^8$; non-ILD *vs*. IPF, P=0.0438; and for combined non-IPF groups *vs*. IPF, P=0.0387). Importantly, we confirmed an increase in EVs in IPF in a second independent cohort of IPF patients and healthy volunteers, although this analysis did not reach statistical significance (Fig. 1H, particles/mL of initial sample: healthy (n=8) $5.7x10^7$±$2.5x10^7$, IPF (n=9) $3.0x10^8$±$3.4x10^8$, P=0.0633). Further analysis of this cohort suggests that EV numbers correlate with lung function (Fig. E2A). Importantly, when combining both cohorts, EVs were significantly increased in IPF compared to non-IPF (Fig. E2B for combined analysis, P=0.0428). Altogether, these results strongly support the notion of enhanced secretion of EVs into the BALF, in both experimental lung fibrosis and human IPF.

WNT-5A is upregulated in BALF-EVs from experimental and human lung fibrosis

EVs exert their function by transporting a variety of mediators and we were wondering whether WNT proteins upregulated in IPF (13, 17) are present on EVs. We found an increase in both WNT-5A mRNA and protein expression in lung homogenates from bleomycin- compared to PBS-treated mice (Fig. 2A and 2B) and upregulated WNT-5A protein in lung homogenates from IPF compared to donor tissue specimens (Fig. 2C), expanding on a previous report (13). To investigate whether WNT secretion is increased in lung fibrosis, we analyzed the expression of the shuttle protein G protein-coupled receptor 177 (GPR177) required for WNT secretion on EVs (18) and found significant increased levels in lung homogenate and BALF from bleomycin-treated mice compared to PBS-treated controls (Fig. 2D and 2E, respectively). Upregulation of GPR177 was further confirmed in lung homogenates from IPF patients compared to donors (Fig. 2F, GPR177 protein: donors 0.35±0.25, IPF 0.48±0.16, P=0.0262).

To study if WNT-5A is indeed secreted on EVs, we looked at WNT-5A in EVs and EV-free supernatants and found enriched WNT-5A in EVs from BALF of fibrotic mouse lungs compared to controls (Fig. 3A). We further found WNT-5A enriched in EVs from supernatants from fibrotic compared to healthy 3D-lung tissue cultures (3D-LTCs), suggesting that these EVs carry WNT-5A under fibrotic conditions and can originate from distal areas of lung tissue (Fig. 3B right panel, WNT-5A protein: PBS 0.12±0.12, Bleo 1.34±0.33, P=0.0004). These results strongly indicate that WNT-5A is transported by EVs in experimental lung fibrosis.

Next, we aimed to elucidate the potential clinical relevance of EV-mediated WNT-5A signaling in IPF. EVs isolated from BALF of non-ILD, non-IPF-ILD, or IPF patients were investigated for the

AJRCCM Articles in Press. Published on 25-July-2018 as 10.1164/rccm.201708-1580OC

expression of WNT-5A along with the EV-enriched proteins TSG101 and CD81, the latter being a tetraspanin involved in EV biogenesis (19). Analyzing the same amount of EV protein, we found increased levels of WNT-5A in EVs from IPF patients when compared to non-IPF EVs (Fig. 3C, WNT-5A expression: non-IPF (n=5) 24.98±9.51, IPF (n=7) 72.09±43.56, P=0.0408). Notably, WNT-5A correlated with CD81 (Fig. 3D, r^2=0.4586, P=0.0156), which is described to be highly expressed on the surface of myofibroblasts (20) and as a marker of a specific EV subpopulation (21), as well as TSG101 (Fig. E3, r^2=0.3762, P=0.0339). Collectively, these results suggest that WNT-5A expression is increased in EVs in IPF and highlight a potential role for EV-bound WNT-5A in intercellular communication during fibrogenesis.

EVs from primary human lung fibroblasts transport WNT-5A and induce fibroblast proliferation

WNT-5A has been recently found to be upregulated in lung fibroblasts in chronic lung disease (22). We thus investigated whether lung fibroblasts secrete EV-associated WNT-5A in the distal lung and isolated EVs from cell culture supernatants from primary human lung fibroblasts (phLFs) and alveolar epithelial type II (phATII) cells (Fig. 4A and B, and Fig. E4). We found an enrichment of WNT-5A in EVs from phLFs compared to EVs from phATII cells (Fig. 4C), suggesting that phLFs are a major source of WNT-5A secretion via EVs in the distal lung.

To address the potential functional implications of EVs, we investigated lung fibroblast proliferation, which has been linked to lung fibrosis (13, 23). We collected EVs from phLFs supernatant and treated phLFs in an autocrine fashion as outlined in detail in M&M. Upon EV treatment, phLFs exhibited a significant increase in their metabolic activity compared to phLFs

treated with EV-free-medium (Fig. 4D, % increase in metabolic activity to control: 0.01µg EVs 19.7±10.4, P=0.0064, 0.5µg EVs 17.6±12.45, P=0.0199). Similarly, we found a significant increase in the number of cells upon EV treatment (Fig. 4E). Notably, the proliferative effect was significantly decreased in disrupted EVs treated with detergent prior to treatment when compared to intact EVs (Fig. 4F). Notably, next to an effect on proliferation, we observed decreased gene expression of the myofibroblast markers *FN1*, *ACTA2, COL1A1* and *TNC* upon EV treatment (Fig. E5). These data indicate that EV-bound WNT-5A promotes a proliferative and not a synthetic cellular phenotype of fibroblasts.

EV-induced proliferation in lung fibroblasts is mediated by WNT-5A

To elucidate whether the effects of EVs on lung fibroblast proliferation are mediated by WNT proteins, we used the inhibitor of WNT production molecule 2 (IWP2), which inhibits overall WNT (24). Pre-treatment of phLFs with IWP2 efficiently decreased WNT-5A secretion in phLFs supernatants (Fig. 5A), and importantly, reduced the proliferative capability of EVs in the recipient phLFs when compared to EVs from vehicle-treated cells (Fig. 5B, % increase in metabolic activity to control: DMSO (vehicle)-EV 45.8±26.6 *vs*. IWP2-EV 27.0±12.3). To further confirm that the proliferative effect was mediated specifically by WNT-5A, we performed siRNA-mediated silencing of WNT-5A in phLFs prior to EV-isolation, which efficiently inhibited WNT-5A secretion while not modifying the expression of the EV-enriched proteins CD81 and TSG10 or the EV secretion profile (Fig. 5C and Fig. E6A and E6B). Notably, WNT-5A-depleted EVs exhibited significant reduced potential to induce proliferation (Fig. 5D, % increase in metabolic activity: scramble siRNA-EV 23.7±15.5 *vs*. WNT-5A siRNA-EV 4.2±9.1, P=0.0401). These results are

AJRCCM Articles in Press. Published on 25-July-2018 as 10.1164/rccm.201708-1580OC

further supported by the finding that WNT-5A silencing in fibroblasts decreased mRNA and protein expression of the cell cycle regulator Cyclin-D1 (Fig. 5E and 5F, respectively). To further confirm these results and exclude off-target effects on EV composition by silencing WNT-5A, we incubated EVs with a WNT-5A neutralizing antibody (WNT-5A-AB) prior to phLFs stimulation, which also decreased the potential of EVs to induce proliferation (Fig. 5G, % increased metabolic activity: EV+IgG 23.8±10.3 *vs*. EV+WNT-5A-AB 10±14.6, P=0.0449). In summary, these results provide evidence that WNT-5A mediates the pro-proliferative effect of EVs on lung fibroblasts.

TGF-β leads to increased WNT5A secretion on EVs and exaggerated proliferation of phLFs

Transforming growth factor (TGF)-β is a key profibrotic cytokine (25) and has recently been reported to induce WNT-5A expression in lung fibroblasts (23). TGF-β stimulation of phLF led to an increased secretion of GPR177 when compared to control-EVs (Fig. 6A), and further increased WNT-5A in EVs (Fig. 6B, WNT5A protein in EVs: ctrl 0.52±0.33, TGFβ 1.68±0.66, P=0.0262). Of note, WNT-5A was particularly enriched in the EV fraction compared to the EV-free supernatant (Fig. 6B). Accordingly, we further observed that TGF-β-derived EVs induced a dose-dependent increase in proliferation (Fig. 6C). This effect was reduced when EVs were incubated with WNT-5A antibody before treatments on EV recipient cells (Fig. 6D).

EVs from BALF of IPF patients increase lung fibroblast proliferation in a WNT-5A-dependent manner

Finally, we wondered if EV-associated WNT-5A in BALF from IPF patients was able to induce fibroblast proliferation. We isolated EVs from different IPF-BALFs and all of them significantly increased phLF proliferation in a dose-dependent manner as measured by total metabolic activity (WST-1 assay), cell counting, as well as by a DNA-synthesis based method (BrdU assay) (Fig. 7A, B and C, respectively). An intact EV structure was required for the effect on proliferation (Fig. 7D). Importantly, the induction of proliferation was significantly decreased when IPF-EVs were pre-incubated with a WNT-5A-AB (Fig. 7E, % increased metabolic activity: EV+IgG 19.3±10 vs EV+W5A-AB 8±13.9, P=0.0284).

AJRCCM Articles in Press. Published on 25-July-2018 as 10.1164/rccm.201708-1580OC

Discussion

Extracellular vesicles (EVs), including exosomes, are secreted membranous vesicles known to drive biological processes by transporting a variety of cargos depending on the cellular source and context (5). Within the last years, EVs have emerged as essential vehicles of both physiological and pathological processes by harboring specific mediators of a (diseased) cell and facilitating communication with other cellular compartments and tissues. Within the lung, our understanding of EV function in disease has just recently begun to grow, with studies highlighting a potential role of EVs in lung cancer and inflammatory lung disease (5, 26, 27). However, besides an observational study detecting increased tissue factor activity in microparticles from BALF from ILD patients (28), EV function in the context of fibrotic processes in the lung, remains unknown. Here, we demonstrate for the first time that 1) EVs, in particular exosomes, are increased in experimental and human pulmonary fibrosis, that 2) WNT-5A can be detected on EVs derived from lung biosamples, and that 3) EVs - in part via WNT-5A - contribute to fibroblast function, and thus disease pathology.

Research in EV biology is highly dependent on standardized protocols for the isolation (15) and proper characterization (29). Here, we largely used serial ultracentrifugation to isolate EVs, which is a state-of-the-art method that does not modify the original sample. We used a variety of methods to characterize EV populations based on morphology, number, size, and expression of EV-enriched proteins in murine and human biosamples. These analyses resulted in the first description of intact exosome enriched-vesicles from BALF fluid of fibrotic murine and human lungs that exhibit functional properties.

EVs are prime mediators for intercellular communication. In IPF, altered cellular crosstalk and communication is a key feature with aberrant epithelial wound healing and fibroblast activation and proliferation (1). Here, we describe that lung fibroblasts are a source of EVs and demonstrated autocrine effects of EVs on fibroblast proliferation, which was enhanced by TGF-β. Similarly, MSC-derived exosomes were found to induce dermal fibroblast proliferation (30). In addition to lung fibroblast proliferation, myofibroblast differentiation occurs during lung remodeling (25). It is thought that fibroblasts exert different phenotypes within a fibrotic lung based on their spatio-temporal distribution. Notably, we did not observe that fibroblast-derived EVs promote myofibroblast differentiation, but rather decrease mRNA levels of myofibroblast markers and as such might promote a proliferative rather than a synthetic phenotype. Similarly, MSC-derived exosomes have also been reported to suppress myofibroblast differentiation (31).

We found that the effect of EVs on fibroblasts was to a large extent mediated by WNT-5A. Disturbed WNT signaling has been implicated in the pathogenesis of several chronic lung diseases, including IPF (12, 17). WNT-5A has been found in IPF fibroblasts (13, 23) and more recently, we found upregulated WNT-5A in early fibrotic like changes in human 3D-LTCs (32). Thus far, most studies have focused on the WNT/β-catenin pathway in IPF, while β-catenin independent WNT signaling is much less explored. While WNT-5A has been largely reported to act β-catenin independent, also β-catenin dependent function can be observed. Nabhan *et al*. recently reported that WNT-5A expressing fibroblasts might induce WNT/β-catenin signaling in ATII cells (33), however, if this effect is mediated by EVs has not been investigated. Importantly, Gross *et al*. discovered that WNT proteins are transported on EVs (11), thus urging us to

AJRCCM Articles in Press. Published on 25-July-2018 as 10.1164/rccm.201708-1580OC

investigate the role of EVs, and in particular EVs carrying WNT proteins, in lung fibrosis. WNT transport on EVs has important implications with respect to the signaling range of WNT proteins, which is thought to be rather short and limited to close neighboring cells. EV-mediated transport can contribute to a larger signaling range of WNT proteins and thus determine the signaling outcome on other cells. WNT-5A has also been reported to promote processes as fibroblast adhesion (34) or invasion (35), as well as epithelial-mesenchymal transition (36), which need to be further studied in the context of EV-associated WNT-5A. Here, we demonstrate that WNT-5A on EVs promotes fibroblast proliferation, and importantly, this effect could not only be attenuated by siRNA-mediated WNT-5A knockdown, but further by antibody-mediated neutralization of WNT-5A on EVs or upon destruction of EV structure. These data corroborate that indeed WNT-5A transported by EVs, is responsible for the observed effects.

We report that fibroblasts are a major source for WNT-5A bound EVs and our data suggest that these contribute to EVs in BALF from IPF patients. However, it is highly likely that other cells contribute to the EV composition of the BALF in IPF, such as epithelial cell or immune cell subpopulations, which thus might alter the functional outcome. Therefore, it will be important to further investigate EV heterogeneity in the BALF of IPF patients, EVs from different cellular sources and their distinct effects on the fibrotic lung cell phenotypes. Here, we provide evidence that WNT-5A bound EVs in IPF BALF contributes to the functional effects, thus suggesting that fibroblast derived EVs can be found in IPF BALF. However, future studies are needed to decipher if BALF EVs from other (fibrotic) lung disease also promote cellular proliferation and if and how other disease-specific mediators are involved in that process. We

recently reported that fibroblast-derived WNT-5A affects alveolar epithelial cell function in COPD (22), highlighting the need to further investigate EV-mediated mesenchymal-epithelial crosstalk. Interestingly, we found that WNT-5A was able to inhibit WNT/β-catenin driven repair in COPD (22, 37). Nevertheless, in IPF, several lines of evidence suggest active WNT/β-catenin signaling in the lung epithelium (38). These probably disease-specific effects on cellular phenotype might be mediated by the distinct composition of EVs or a specific surface receptor profile on the recipient cell. It has been demonstrated that EVs are taken up by specific cell types due to a distinct integrin expression pattern (39). Another intriguing hypothesis is that EVs - depending on the microenvironment - harbor diverse components of a specific pathway, including specific signaling receptors that enable the recipient cell to exert novel functions and phenotypes.

Our work further raises the more general question whether EVs promote lung fibrosis development or might have a protective role *in vivo*. Notably, several studies to date indicate that EVs play versatile roles depending on the (disease) specific microenvironment with MSC derived-EVs able to facilitate tissue repair (31, 40, 41), and modulating myofibroblast differentiation in IPF fibroblasts (42), while others have suggested proinflammatory roles (43)(44)(27). Moreover, EVs derived from lung cancer cells modulate the tumor microenvironment and can promote tumor metastasis (26, 45, 46). Thus, additional studies inhibiting EV secretion or altering EV composition *in vivo*, ideally in a cell-specific manner, are needed to elucidate the potential damaging *versus* resolving role of EVs in pulmonary fibrosis.

AJRCCM Articles in Press. Published on 25-July-2018 as 10.1164/rccm.201708-1580OC

We investigated a limited amount of patient samples in this study to provide first evidence that EVs are increased in IPF and carry important functional mediator, such as WNT-5A. A comprehensive characterization of EVs requires large amount of biosamples, which restricted the overall number of patient samples we could investigate in this study. While both independent cohorts showed similar results, future investigations of larger cohorts will be essential to further confirm the potential correlation of EVs with clinical parameters, such as lung function. These studies will need to consider the heterogeneity of the BALF samples (such as differential cell counts), include different ILDs, and allow adjustment for parameter as age and gender**.** Furthermore, it will be interesting to explore the potential role of EVs as blood biomarkers for ILDs (47), and other EV components such as DNA, mRNA or microRNAs that might contribute to disease (5, 26, 48).

In summary, our present study reports for the first time that EVs can be found in in experimental and human pulmonary fibrosis, carry fibrotic mediator such as WNT-5A, and contribute to fibrogenesis. Further investigations of EVs in this devastating disease to better understand the contribution to fibrotic pathomechanisms, as well as to elucidate their potential as therapeutic and biomarkers are warranted.

Acknowledgments

The authors are very grateful to all members of the Königshoff Laboratory for stimulating and fruitful discussions. We are thankful to Anastasia van den Berg, Julia Kipp, Nadine Adam, Rabea Imker, Maria Magdalena Stein (CPC Munich) and Gabriele Mettenleiter (Research Unit Analytical Pathology, Helmholtz Zentrum München as well as Dr. Jennifer Bourne (Electron Microscopy Center, UC Denver AMC) for excellent technical assistance. We thank Dr. Katharina Heinzelmann and the MLT team for phLFs isolation and the Universitätsklinikum Gießen, the Asklepios Fachkliniken München-Gauting and the CPC Bioarchive, especially to Ina Koch, Anja Stowasser and Dr. Annika Frank, for providing the lung tissue and BALF from human patients. Finally, we want to thank Dr. Kerstin Stemmer and Michaela Bauer for guidance on EV isolation and Dr. Timothy Boyd and the Rocky Mountain Alzheimer's Disease Center for advice and help with the nanoparticle tracking analysis.

AJRCCM Articles in Press. Published on 25-July-2018 as 10.1164/rccm.201708-1580OC

References

1. Fernandez IE, Eickelberg O. The impact of TGF-beta on lung fibrosis: from targeting to biomarkers. *Proceedings of the American Thoracic Society* 2012; 9: 111-116.
2. White ES, Lazar MH, Thannickal VJ. Pathogenetic mechanisms in usual interstitial pneumonia/idiopathic pulmonary fibrosis. *The Journal of pathology* 2003; 201: 343-354.
3. Colombo M, Raposo G, Thery C. Biogenesis, secretion, and intercellular interactions of exosomes and other extracellular vesicles. *Annual review of cell and developmental biology* 2014; 30: 255-289.
4. Yanez-Mo M, Siljander PR, Andreu Z, Zavec AB, Borras FE, Buzas EI, Buzas K, Casal E, Cappello F, Carvalho J, Colas E, Cordeiro-da Silva A, Fais S, Falcon-Perez JM, Ghobrial IM, Giebel B, Gimona M, Graner M, Gursel I, Gursel M, Heegaard NH, Hendrix A, Kierulf P, Kokubun K, Kosanovic M, Kralj-Iglic V, Kramer-Albers EM, Laitinen S, Lasser C, Lener T, Ligeti E, Line A, Lipps G, Llorente A, Lotvall J, Mancek-Keber M, Marcilla A, Mittelbrunn M, Nazarenko I, Nolte-'t Hoen EN, Nyman TA, O'Driscoll L, Olivan M, Oliveira C, Pallinger E, Del Portillo HA, Reventos J, Rigau M, Rohde E, Sammar M, Sanchez-Madrid F, Santarem N, Schallmoser K, Ostenfeld MS, Stoorvogel W, Stukelj R, Van der Grein SG, Vasconcelos MH, Wauben MH, De Wever O. Biological properties of extracellular vesicles and their physiological functions. *Journal of extracellular vesicles* 2015; 4: 27066.
5. Nana-Sinkam SP, Acunzo M, Croce CM, Wang K. Extracellular Vesicle Biology in the Pathogenesis of Lung Disease. *American journal of respiratory and critical care medicine* 2017; 196: 1510-1518.
6. Kubo H. Extracellular Vesicles in Lung Disease. *Chest* 2018; 153: 210-216.
7. Szul T, Bratcher PE, Fraser KB, Kong M, Tirouvanziam R, Ingersoll S, Sztul E, Rangarajan S, Blalock JE, Xu X, Gaggar A. Toll-Like Receptor 4 Engagement Mediates Prolyl Endopeptidase Release from Airway Epithelia via Exosomes. *American journal of respiratory cell and molecular biology* 2016; 54: 359-369.
8. Konigshoff M, Balsara N, Pfaff EM, Kramer M, Chrobak I, Seeger W, Eickelberg O. Functional Wnt signaling is increased in idiopathic pulmonary fibrosis. *PLoS One* 2008; 3: e2142.
9. Chilosi M, Poletti V, Zamo A, Lestani M, Montagna L, Piccoli P, Pedron S, Bertaso M, Scarpa A, Murer B, Cancellieri A, Maestro R, Semenzato G, Doglioni C. Aberrant Wnt/beta-catenin pathway activation in idiopathic pulmonary fibrosis. *Am J Pathol* 2003; 162: 1495-1502.
10. Selman M, Pardo A, Kaminski N. Idiopathic pulmonary fibrosis: aberrant recapitulation of developmental programs? *PLoS medicine* 2008; 5: e62.
11. Gross JC, Chaudhary V, Bartscherer K, Boutros M. Active Wnt proteins are secreted on exosomes. *Nat Cell Biol* 2012; 14: 1036-1045.
12. Baarsma HA, Konigshoff M. 'WNT-er is coming': WNT signalling in chronic lung diseases. *Thorax* 2017; 72: 746-759.
13. Vuga LJ, Ben-Yehudah A, Kovkarova-Naumovski E, Oriss T, Gibson KF, Feghali-Bostwick C, Kaminski N. WNT5A is a regulator of fibroblast proliferation and resistance to apoptosis. *American journal of respiratory cell and molecular biology* 2009; 41: 583-589.
14. Medina AM, Vierkotten S, Lehmann M, Wagner DE, Baarsma H, Hofer T, Frankerberger M, Behr J, Aichler M, Walch A, 1 MK. WNT5A Is Secreted by Extracellular Vesicles in Pulmonary Fibrosis and Increases Fibroblasts Proliferation [abstract]. *American journal of respiratory and critical care medicine* 2017; 195: A7565.
15. Thery C, Amigorena S, Raposo G, Clayton A. Isolation and characterization of exosomes from cell culture supernatants and biological fluids. *Current protocols in cell biology / editorial board, Juan S Bonifacino [et al]* 2006; Chapter 3: Unit 3 22.

16. Yoshioka Y, Konishi Y, Kosaka N, Katsuda T, Kato T, Ochiya T. Comparative marker analysis of extracellular vesicles in different human cancer types. *Journal of extracellular vesicles* 2013; 2.
17. Burgy O, Konigshoff M. The WNT signaling pathways in wound healing and fibrosis. *Matrix Biol* 2018.
18. Koles K, Budnik V. Exosomes go with the Wnt. *Cellular logistics* 2012; 2: 169-173.
19. Andreu Z, Yanez-Mo M. Tetraspanins in extracellular vesicle formation and function. *Frontiers in immunology* 2014; 5: 442.
20. Akamatsu T, Arai Y, Kosugi I, Kawasaki H, Meguro S, Sakao M, Shibata K, Suda T, Chida K, Iwashita T. Direct isolation of myofibroblasts and fibroblasts from bleomycin-injured lungs reveals their functional similarities and differences. *Fibrogenesis & tissue repair* 2013; 6: 15.
21. Kowal J, Arras G, Colombo M, Jouve M, Morath JP, Primdal-Bengtson B, Dingli F, Loew D, Tkach M, Thery C. Proteomic comparison defines novel markers to characterize heterogeneous populations of extracellular vesicle subtypes. *Proceedings of the National Academy of Sciences of the United States of America* 2016; 113: E968-977.
22. Baarsma HA, Skronska-Wasek W, Mutze K, Ciolek F, Wagner DE, John-Schuster G, Heinzelmann K, Gunther A, Bracke KR, Dagouassat M, Boczkowski J, Brusselle GG, Smits R, Eickelberg O, Yildirim AO, Konigshoff M. Noncanonical WNT-5A signaling impairs endogenous lung repair in COPD. *The Journal of experimental medicine* 2017; 214: 143-163.
23. Newman DR, Sills WS, Hanrahan K, Ziegler A, Tidd KM, Cook E, Sannes PL. Expression of WNT5A in Idiopathic Pulmonary Fibrosis and Its Control by TGF-beta and WNT7B in Human Lung Fibroblasts. *The journal of histochemistry and cytochemistry : official journal of the Histochemistry Society* 2016; 64: 99-111.
24. Dodge ME, Moon J, Tuladhar R, Lu J, Jacob LS, Zhang LS, Shi H, Wang X, Moro E, Mongera A, Argenton F, Karner CM, Carroll TJ, Chen C, Amatruda JF, Lum L. Diverse chemical scaffolds support direct inhibition of the membrane-bound O-acyltransferase porcupine. *The Journal of biological chemistry* 2012; 287: 23246-23254.
25. Chambers RC, Mercer PF. Mechanisms of alveolar epithelial injury, repair, and fibrosis. *Annals of the American Thoracic Society* 2015; 12 Suppl 1: S16-20.
26. Parimon T, Brauer R, Schlesinger SY, Xie T, Jiang D, Ge L, Huang Y, Birkland TP, Parks WC, Habiel DM, Hogaboam CM, Gharib SA, Deng N, Liu Z, Chen P. Syndecan-1 Controls Lung Tumorigenesis by Regulating miRNAs Packaged in Exosomes. *The American journal of pathology* 2018; 188: 1094-1103.
27. Speth JM, Bourdonnay E, Penke LR, Mancuso P, Moore BB, Weinberg JB, Peters-Golden M. Alveolar Epithelial Cell-Derived Prostaglandin E2 Serves as a Request Signal for Macrophage Secretion of Suppressor of Cytokine Signaling 3 during Innate Inflammation. *Journal of immunology* 2016; 196: 5112-5120.
28. Novelli F, Neri T, Tavanti L, Armani C, Noce C, Falaschi F, Bartoli ML, Martino F, Palla A, Celi A, Paggiaro P. Procoagulant, tissue factor-bearing microparticles in bronchoalveolar lavage of interstitial lung disease patients: an observational study. *PLoS One* 2014; 9: e95013.
29. Coumans FAW, Brisson AR, Buzas EI, Dignat-George F, Drees EEE, El-Andaloussi S, Emanueli C, Gasecka A, Hendrix A, Hill AF, Lacroix R, Lee Y, van Leeuwen TG, Mackman N, Mager I, Nolan JP, van der Pol E, Pegtel DM, Sahoo S, Siljander PRM, Sturk G, de Wever O, Nieuwland R. Methodological Guidelines to Study Extracellular Vesicles. *Circulation research* 2017; 120: 1632-1648.
30. McBride JD, Rodriguez-Menocal L, Guzman W, Candanedo A, Garcia-Contreras M, Badiavas EV. Bone Marrow Mesenchymal Stem Cell-Derived CD63(+) Exosomes Transport Wnt3a Exteriorly and Enhance Dermal Fibroblast Proliferation, Migration, and Angiogenesis In Vitro. *Stem cells and development* 2017; 26: 1384-1398.

AJRCCM Articles in Press. Published on 25-July-2018 as 10.1164/rccm.201708-1580OC

31. Fang S, Xu C, Zhang Y, Xue C, Yang C, Bi H, Qian X, Wu M, Ji K, Zhao Y, Wang Y, Liu H, Xing X. Umbilical Cord-Derived Mesenchymal Stem Cell-Derived Exosomal MicroRNAs Suppress Myofibroblast Differentiation by Inhibiting the Transforming Growth Factor-beta/SMAD2 Pathway During Wound Healing. *Stem cells translational medicine* 2016; 5: 1425-1439.
32. Alsafadi HN, Staab-Weijnitz CA, Lehmann M, Lindner M, Peschel B, Konigshoff M, Wagner DE. An ex vivo model to induce early fibrosis-like changes in human precision-cut lung slices. *Am J Physiol Lung Cell Mol Physiol* 2017; 312: L896-L902.
33. Nabhan AN, Brownfield DG, Harbury PB, Krasnow MA, Desai TJ. Single-cell Wnt signaling niches maintain stemness of alveolar type 2 cells. *Science* 2018; 359: 1118-1123.
34. Kawasaki A, Torii K, Yamashita Y, Nishizawa K, Kanekura K, Katada M, Ito M, Nishimoto I, Terashita K, Aiso S, Matsuoka M. Wnt5a promotes adhesion of human dermal fibroblasts by triggering a phosphatidylinositol-3 kinase/Akt signal. *Cellular signalling* 2007; 19: 2498-2506.
35. Waster P, Rosdahl I, Gilmore BF, Seifert O. Ultraviolet exposure of melanoma cells induces fibroblast activation protein-alpha in fibroblasts: Implications for melanoma invasion. *International journal of oncology* 2011; 39: 193-202.
36. Gujral TS, Chan M, Peshkin L, Sorger PK, Kirschner MW, MacBeath G. A noncanonical Frizzled2 pathway regulates epithelial-mesenchymal transition and metastasis. *Cell* 2014; 159: 844-856.
37. Kneidinger N, Yildirim AO, Callegari J, Takenaka S, Stein MM, Dumitrascu R, Bohla A, Bracke KR, Morty RE, Brusselle GG, Schermuly RT, Eickelberg O, Konigshoff M. Activation of the WNT/beta-catenin pathway attenuates experimental emphysema. *American journal of respiratory and critical care medicine* 2011; 183: 723-733.
38. Aumiller V, Balsara N, Wilhelm J, Gunther A, Konigshoff M. WNT/beta-catenin signaling induces IL-1beta expression by alveolar epithelial cells in pulmonary fibrosis. *American journal of respiratory cell and molecular biology* 2013; 49: 96-104.
39. Hoshino A, Costa-Silva B, Shen TL, Rodrigues G, Hashimoto A, Tesic Mark M, Molina H, Kohsaka S, Di Giannatale A, Ceder S, Singh S, Williams C, Soplop N, Uryu K, Pharmer L, King T, Bojmar L, Davies AE, Ararso Y, Zhang T, Zhang H, Hernandez J, Weiss JM, Dumont-Cole VD, Kramer K, Wexler LH, Narendran A, Schwartz GK, Healey JH, Sandstrom P, Labori KJ, Kure EH, Grandgenett PM, Hollingsworth MA, de Sousa M, Kaur S, Jain M, Mallya K, Batra SK, Jarnagin WR, Brady MS, Fodstad O, Muller V, Pantel K, Minn AJ, Bissell MJ, Garcia BA, Kang Y, Rajasekhar VK, Ghajar CM, Matei I, Peinado H, Bromberg J, Lyden D. Tumour exosome integrins determine organotropic metastasis. *Nature* 2015; 527: 329-335.
40. Katsuda T, Ochiya T. Molecular signatures of mesenchymal stem cell-derived extracellular vesicle-mediated tissue repair. *Stem cell research & therapy* 2015; 6: 212.
41. Cruz FF, Borg ZD, Goodwin M, Sokocevic D, Wagner DE, Coffey A, Antunes M, Robinson KL, Mitsialis SA, Kourembanas S, Thane K, Hoffman AM, McKenna DH, Rocco PR, Weiss DJ. Systemic Administration of Human Bone Marrow-Derived Mesenchymal Stromal Cell Extracellular Vesicles Ameliorates Aspergillus Hyphal Extract-Induced Allergic Airway Inflammation in Immunocompetent Mice. *Stem cells translational medicine* 2015; 4: 1302-1316.
42. Shentu TP, Huang TS, Cernelc-Kohan M, Chan J, Wong SS, Espinoza CR, Tan C, Gramaglia I, van der Heyde H, Chien S, Hagood JS. Thy-1 dependent uptake of mesenchymal stem cell-derived extracellular vesicles blocks myofibroblastic differentiation. *Scientific reports* 2017; 7: 18052.
43. Kulshreshtha A, Ahmad T, Agrawal A, Ghosh B. Proinflammatory role of epithelial cell-derived exosomes in allergic airway inflammation. *The Journal of allergy and clinical immunology* 2013; 131: 1194-1203, 1203 e1191-1114.

44. Qazi KR, Torregrosa Paredes P, Dahlberg B, Grunewald J, Eklund A, Gabrielsson S. Proinflammatory exosomes in bronchoalveolar lavage fluid of patients with sarcoidosis. *Thorax* 2010; 65: 1016-1024.
45. Fabbri M, Paone A, Calore F, Galli R, Gaudio E, Santhanam R, Lovat F, Fadda P, Mao C, Nuovo GJ, Zanesi N, Crawford M, Ozer GH, Wernicke D, Alder H, Caligiuri MA, Nana-Sinkam P, Perrotti D, Croce CM. MicroRNAs bind to Toll-like receptors to induce prometastatic inflammatory response. *Proceedings of the National Academy of Sciences of the United States of America* 2012; 109: E2110-2116.
46. Rahman MA, Barger JF, Lovat F, Gao M, Otterson GA, Nana-Sinkam P. Lung cancer exosomes as drivers of epithelial mesenchymal transition. *Oncotarget* 2016; 7: 54852-54866.
47. Ruiz-Lopez L, Blancas I, Garrido JM, Mut-Salud N, Moya-Jodar M, Osuna A, Rodriguez-Serrano F. The role of exosomes on colorectal cancer: A review. *J Gastroenterol Hepatol* 2018; 33: 792-799.
48. Schneider DJ, Speth JM, Penke LR, Wettlaufer SH, Swanson JA, Peters-Golden M. Mechanisms and modulation of microvesicle uptake in a model of alveolar cell communication. *The Journal of biological chemistry* 2017; 292: 20897-20910.

AJRCCM Articles in Press. Published on 25-July-2018 as 10.1164/rccm.201708-1580OC

Table1

Characteristics	Control, non-ILD*	COP	HP	IPF	All
N =	12	2	5	16	35
Male gender, no. (%)	3 (25%)	1 (50%)	3 (60%)	10 (63%)	17 (49%)
Age (years ± SD)	57.4 ± 14.3	73 ± 1.5	55.6 ± 5.9	68.7 ± 11.0	63.8 ± 12.3
FVC (L ± SD)	4.9 ± 0.4	5.0 ± 0.8	4.2 ± 0.7	3.4 ± 0.7	3.8 ± 0.8
DLCO (% pred ± SD)	77.1 ± 10.7	82 ± 11	43.9 ± 7.16	54.3 ± 12.6	60.3 ± 18.5

Table1. Characteristic of the patients included in the Munich cohort.

Footnotes: *control non-ILD group: diagnostic evaluation of unclear cough (n=10), Previous breast cancer metastasis (n=1) and post-transplantation (n=1). All with no signs of ILD. Abbreviations; COP: Cryptogenic organizing pneumonia, HP: Hypersensitivity pneumonitis, FVC: Forced vital capacity, DLCO: diffusing capacity of the lung for carbon monoxide.

Table 2

Characteristics	Healthy volunteers	IPF	All
n=	8	9	17
Male gender, no. (%)	4 (50%)	9 (100%)	13 (76%)
Age (years ± SD)	57.5 ± 6.7	71.1 ± 3.3	64.7 ± 8.6
FVC (L ± SD)	4.3 ± 1.0	3.6 ± 1.2	4.0 ± 1.1
DLCO (% pred ± SD)	no data	47.9 ± 12.9	-

Table2. Characteristic of the patients included in the UCSF cohort.

Footnotes: Abbreviations; FVC: Forced vital capacity, DLCO: diffusing capacity of the lung for carbon monoxide.

AJRCCM Articles in Press. Published on 25-July-2018 as 10.1164/rccm.201708-1580OC

Figure legends

Figure 1. Extracellular Vesicle (EV) secretion is increased in experimental and human pulmonary fibrosis. (A) Scheme of the protocols used for the isolation of EVs in bronchoalveolar lavage fluid (BALF) and cell culture (supernatant (SN)). Abbreviations: extracellular vesicle pellet: EV-P, extracellular vesicle-free supernatant: EV-free-SN. (B) Representative transmission electron microscopy image of EVs isolated from BALF of mice treated with PBS (vehicle) or bleomycin (BALF-EV PBS, BALF-EV Bleo, respectively). BALF was collected at day 14 post-instillation. Arrows indicate exosomes and arrowheads indicate microvesicles. (C) Total protein quantification in EVs isolated from BALF from PBS- and bleomycin-treated mice (n=8 per group). (D) Histogram showing the results of nanoparticle tracking analysis (NTA) performed on same samples as in B (measurements in triplicates; n=3 per group) (left), graph of the vesicles grouped in exosomes (Exo; 30-200nm) or microvesicles (MVs; 200-2000) (middle), and statistics for the exosomal fraction (right). Data is represented as particles/mL of EV fraction. (E) Representative transmission electron microscopy images of EVs isolated from BALF from non-ILD or IPF patients. (F) Total protein quantification in EV-pellets isolated from BALF from non-ILD/non-IPF-ILD (n=12/7) and IPF (n=16) patients. (G) NTA analysis determining the size and number of the vesicles isolated from BALF from non-ILD (n=7), non-IPF-ILD (n=6), and IPF (n=4) patients. Measurements were done in 5 replicates (right), graph representing the results in Exo (30-200nm) versus MVs (200-1000nm) (middle), and statistics representing the amount of EVs in in the three groups (left). Data is represented as particle/mL related to initial sample. (H) Quantification of EVs isolated from BALF of healthy volunteers or patients with IPF from a

second cohort of patients (Table 2). Data is represented as particle/mL related to initial sample. All EVs were isolated by ultracentrifugation. Student's *t*-test; *p<0.05, ***p<0.001.

Figure 2. WNT-5A is upregulated in lung homogenates from experimental and human pulmonary fibrosis. (A-B) Expression of WNT-5A (A) protein and (B) mRNA level in lung homogenates from PBS- or bleomycin-treated mice (n=3-8 mice per group). (C) Protein analysis of WNT-5A expression in lung homogenates from donors and IPF patients and subsequent densitometry analysis (n=6 per group). (D-E) Expression of the WNT shuttle protein GPR177 in (D) lung homogenates and (E) BALF from PBS- or bleomycin-treated mice (n=3 per group). Ponceau S staining was used as loading confirmation. (F) Protein expression of GPR177 in lung homogenates from donors (n=7) and IPF (n=7) patients and subsequent densitometry. Student´s *t* test was used in all statistics; *p<0.05, **p<0.01, ***p<0.001.

Figure 3. Increased WNT-5A is carried on EVs in pulmonary fibrosis. (A-B) Analysis of TSG101 and WNT-5A in (A) whole EV-Pellets from BALF (n=3 per group) and (B) EV-Pellets isolated from 3D-lung slices culture supernatants from PBS- and bleomycin-treated mice by ExoQuick® (n=4 per group). Equal amount of EV pellets was loaded (10ug). Densitometry analysis of panel B: WNT-5A expression relative to Ponceau (right panel), Student's *t* test. (C) Protein analysis of EV-enriched proteins TSG101 and CD81, as well as WNT-5A in EV-P isolated by ultracentrifugation in BALF from non-ILD (n=3), IPF (n=7) and Hypersensitivity Pneumonitis (HP) (n=2), and corresponding densitometry of WNT-5A relative to Ponceau, Student's *t* test. (D) Correlation between WNT-5A and CD81 expression (dots represent single values; linear regression test). Ponceau S staining was used for loading confirmation. *p<0.05, **p<0.01.

AJRCCM Articles in Press. Published on 25-July-2018 as 10.1164/rccm.201708-1580OC

Figure 4. Human lung fibroblasts are a source of EVs, which induce lung fibroblast proliferation. (A) Representative transmission electron microscopy images of EVs isolated from (A) primary human lung fibroblasts (phLFBs) and (B) primary human epithelial type II (phATII) cell culture supernatants. (C) Comparison of the EV-enriched proteins TSG101 and CD81, as well as WNT-5A, in equally-loaded EV Pellets isolated from phLFBs or phATII cell culture supernatants. Ponceau S staining was used as loading control. (D-E) Assessment of proliferation by WST-1 assay (D) or cell counting (E) of phLFs stimulated with EVs at the indicating concentrations for 48h (n=3 and n=6 respectively; 1way ANOVA; Dunnett´s post-test; $p<0.05$). (F) Proliferation analysis by WST-1 assay in phLFs stimulated with autocrine EVs alone (EV) or pre-treated with detergent (EV+triton). N=3 per group. Paired Student's *t* test; $p<0.05$.

Figure 5. Human lung fibroblast-derived EV induced lung fibroblast proliferation is WNT-5A dependent. (A) Detection of WNT-5A protein in phLFs supernatants after treatment with inhibitor of WNT protein secretion IWP2 or DMSO as control (data show n=3 independent experiments). (B) Proliferation analysis by WST1-assay after 48 h stimulation of phLFs with 0.5 µg prot./ml of autocrine EVs isolated in phLFs following treatment with IWP2 (IWP-EV) or DMSO control (DMSO-EV) (n=4 per group). (C) Analysis of WNT-5A protein in supernatants from phLFs treated with WNT-5A siRNA (siW5A) or scrambled siRNA control (scr) for 24h. Ponceau S staining was used for loading confirmation of the supernatants. (D) Proliferation assay after 48 h stimulation of phLFs with 0.5 µg protein/ml of EVs isolated from phLFs after treatment with WNT-5A siRNA (siW5A-EV) or scrambled (scr-EV) (n=3 per group). (E) mRNA levels and (F) protein expression of cyclin D1 gene (CCND1) after 24 h stimulation of phLFs with siWNT-5A

(siW5A) or scrambled siRNA (scr) as control. n=3 per group. (G) Proliferation assay after 48 h stimulation of phLFs with 0.01 µg proein./ml of autocrine EVs that have been incubated with 1 µg of WNT-5A neutralizing antibody (EV+W5A AB) or IgG control (EV+IgG) (n=3 per group).. Paired Student's *t* test for all; P<0.05.

Figure 6: TGF-β induces WNT-5A expression in phLFs-EVs. (A) Protein levels of secreted GPR177 in the supernatants of phLFs after stimulation with TGF-β and subsequent densitometry relative to Ponceau. n=3 per group, paired Student's *t* test; p<0.05. (B) Protein expression analysis of endoplasmatic reticulum protein Calreticulin, the EV-enriched protein CD81 and WNT-5A in: cell lysates (CL), pure supernatants (pSN), EV-Pellets (EV-P) and EV-free-supernatants (EV-free-SN) from phLFBs treated with TGF-β (2ng/ml) for 48 h, and respective densitometry analysis of WNT-5A relative to CD81 (graph represents 3 independent experiments; paired Student's *t* test; p<0.05). (C-D) Assessment of proliferation by WST-1 assay of phLFs stimulated for 48h with (C) EVs from TGF-β-stimulated phLFs at the indicating concentrations (n=4; 1way ANOVA, Dunnett's post-test (*), Bonferroni post-test (#); p<0.05), and (D) same EVs incubated with WNT-5A antibody, paired Student's *t* test; p<0.05.

Figure 7: WNT-5A on BALF-EVs from IPF patients drive lung fibroblast proliferation. Assessment of proliferation by (A) WST-1 assay, (B) cell counting or (C) BrdU assay of phLFs stimulated with EVs isolated from human IPF-BALF at the indicating concentrations for 48h (1way ANOVA, Dunnett´s post-test, n=7, n=3 and n=8; respectively). (D) Proliferation analysis by WST-1 assay in phLFs stimulated with IPF-EVs alone (EV) or pre-treated with detergent (EV+triton). N=4 per group. Paired Student's *t* test; p<0.05. (E) Proliferation assay by WST-1 of donor phLFs after 48h

AJRCCM Articles in Press. Published on 25-July-2018 as 10.1164/rccm.201708-1580OC

treatment with human IPF-BALF-EVs incubated with WNT-5A antibody (W5a AB) or IgG control (n=7 per group; paired Student's *t* test; $p<0.05$).

Figure 1

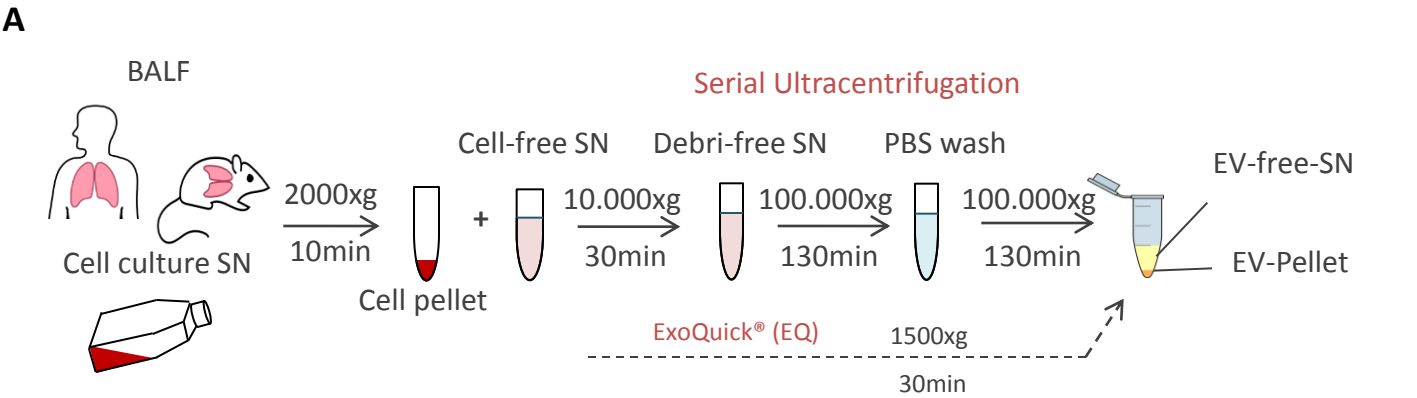

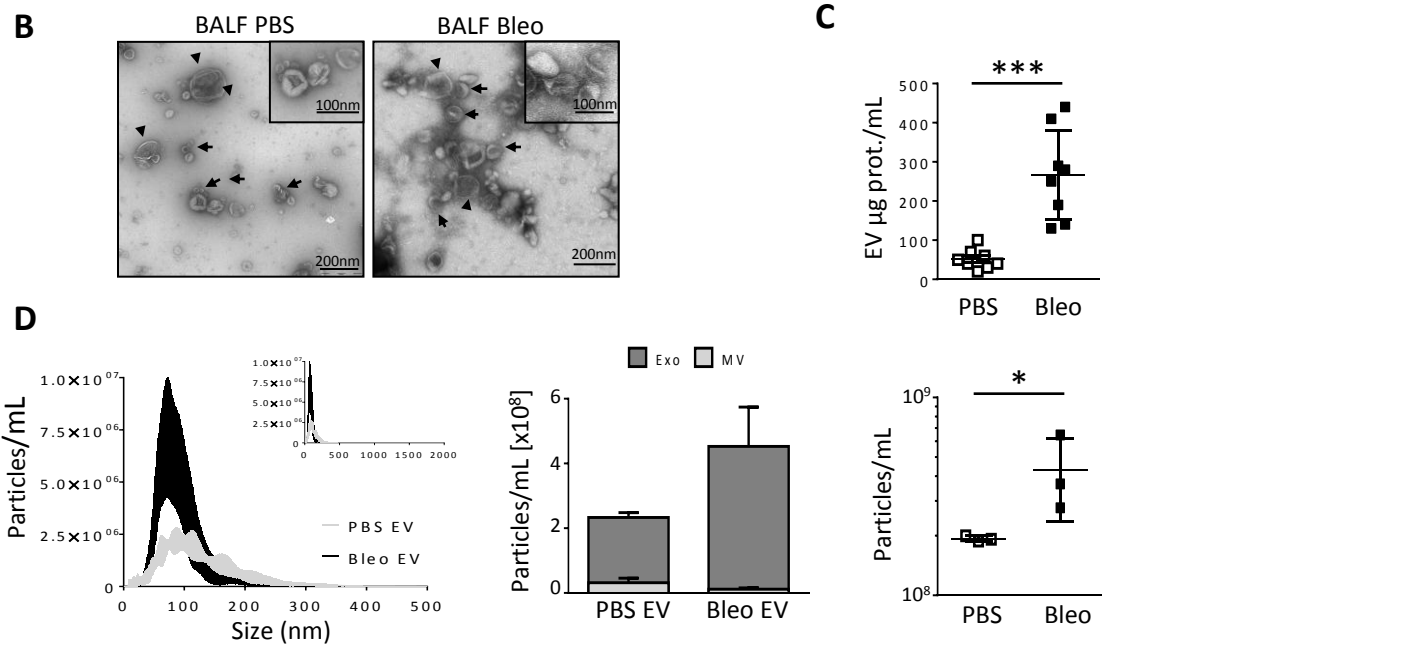

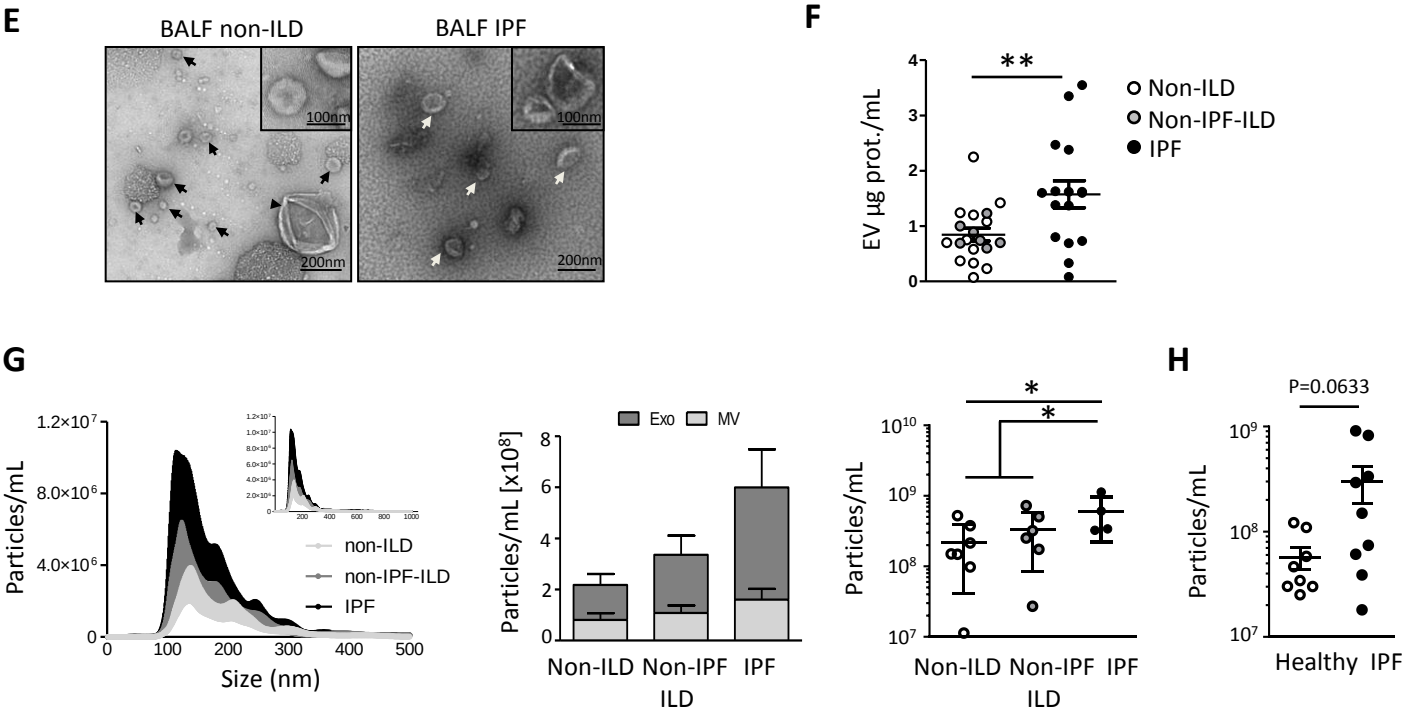

AJRCCM Articles in Press. Published on 25-July-2018 as 10.1164/rccm.201708-1580OC

Figure 2

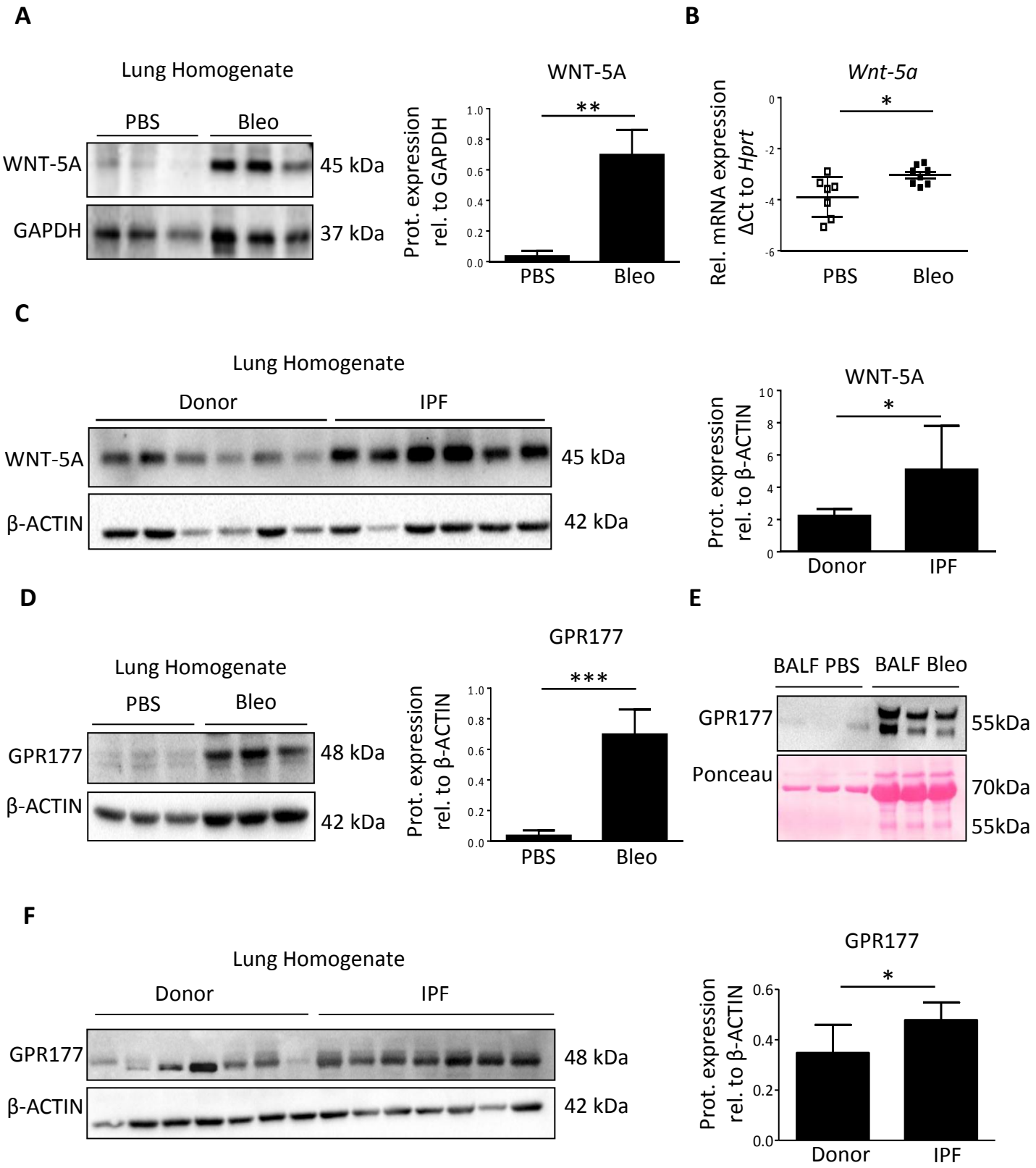

Figure 3

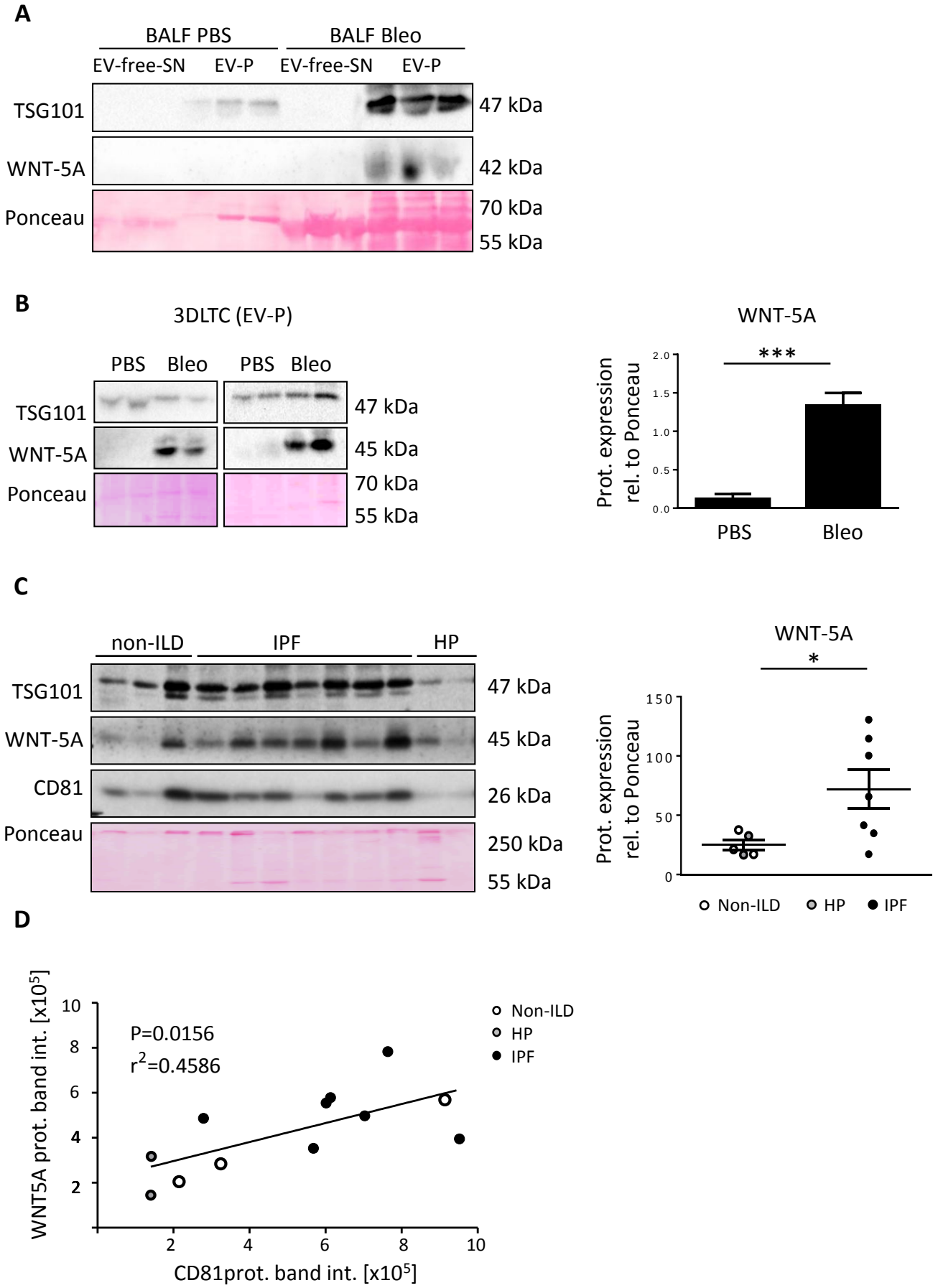

AJRCCM Articles in Press. Published on 25-July-2018 as 10.1164/rccm.201708-1580OC

Figure 4

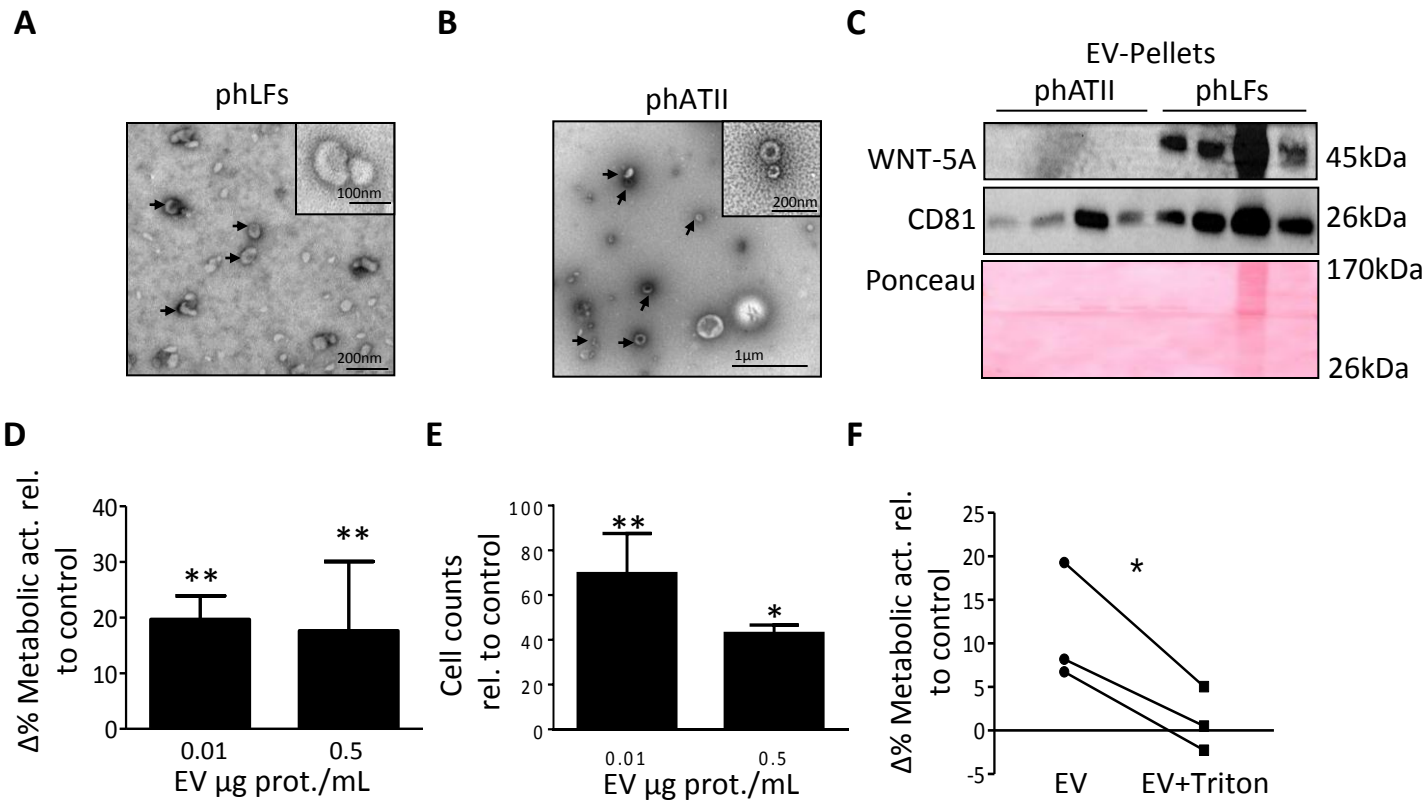

Figure 5

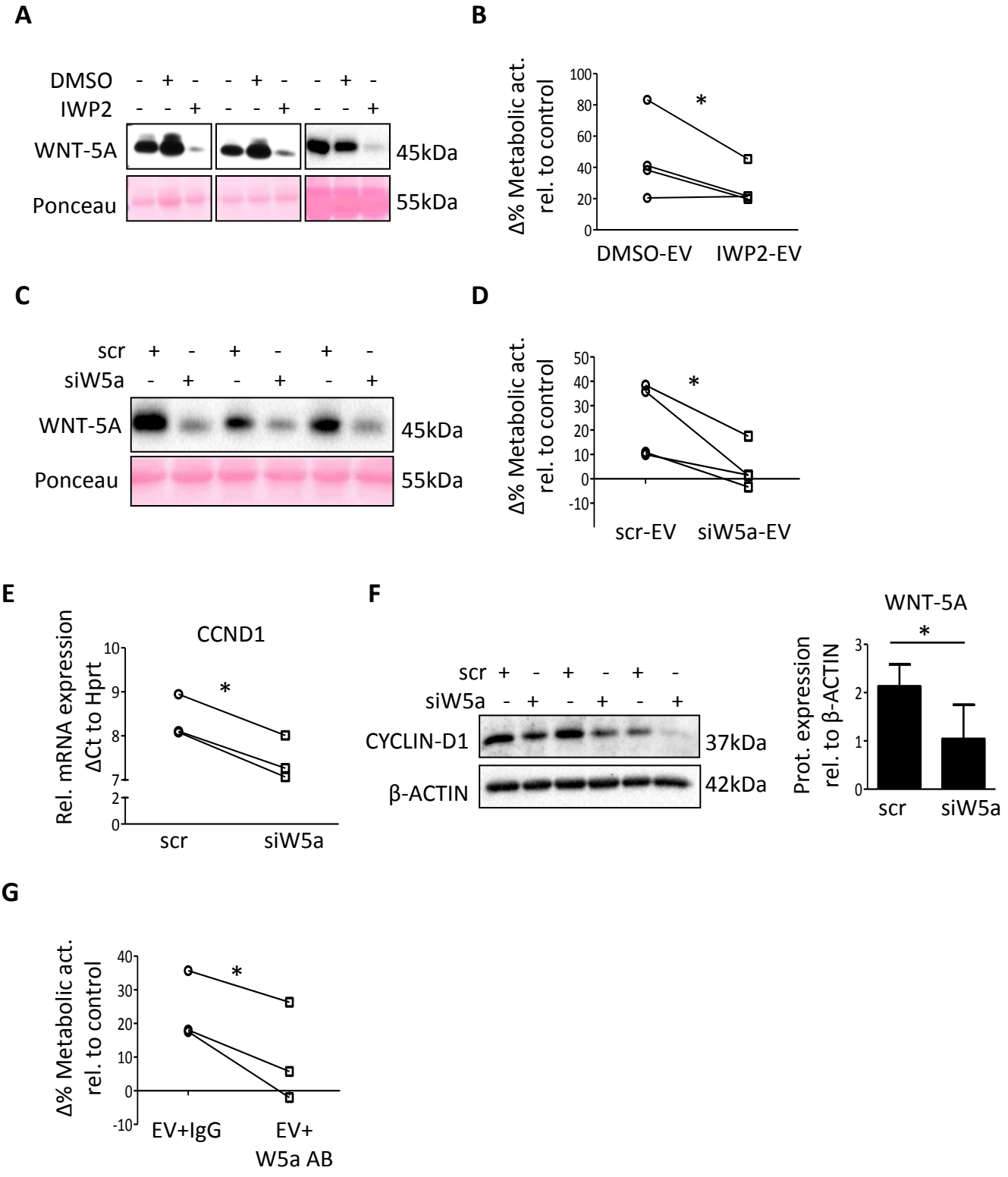

AJRCCM Articles in Press. Published on 25-July-2018 as 10.1164/rccm.201708-1580OC

Figure 6

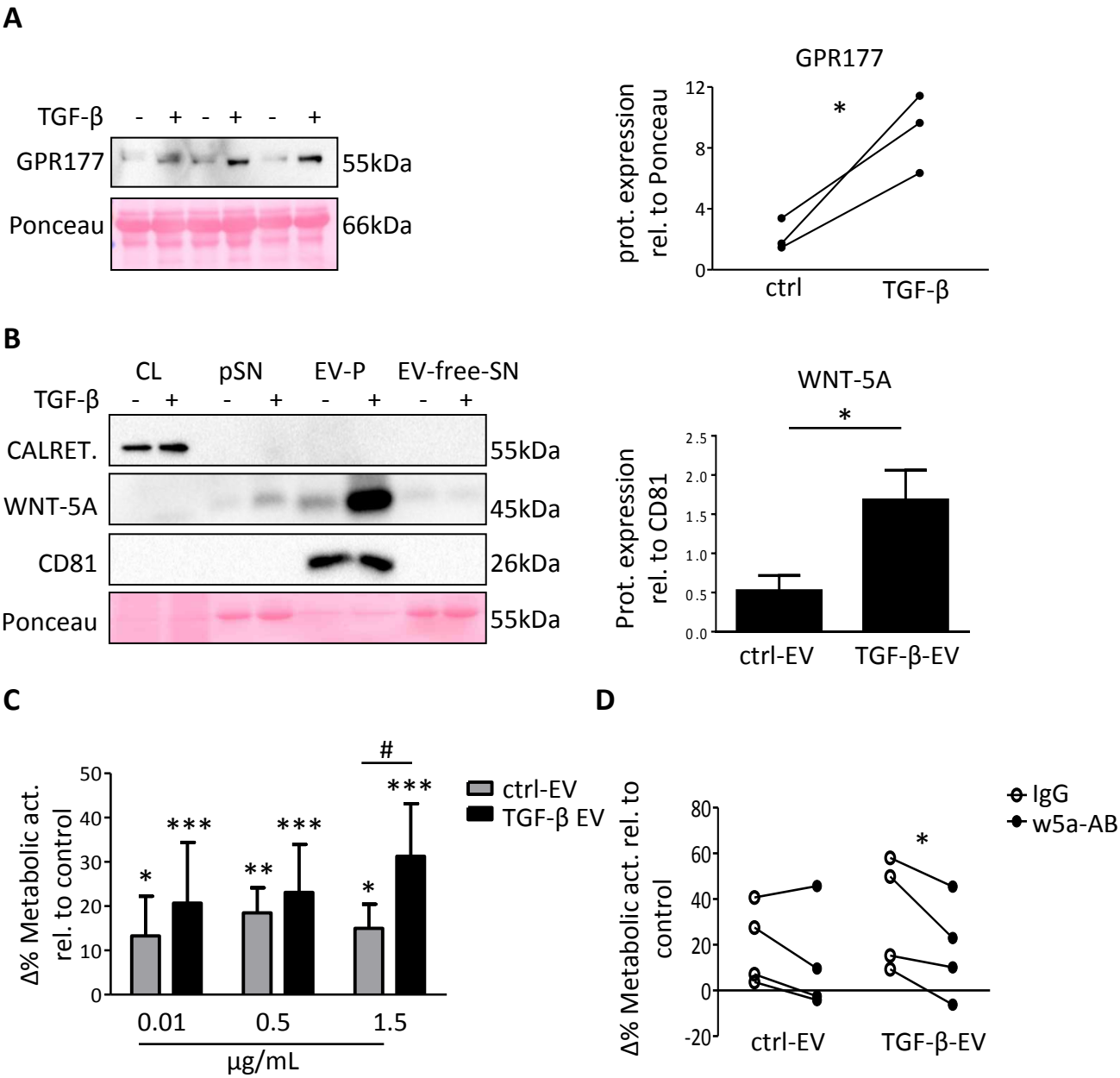

Figure 7

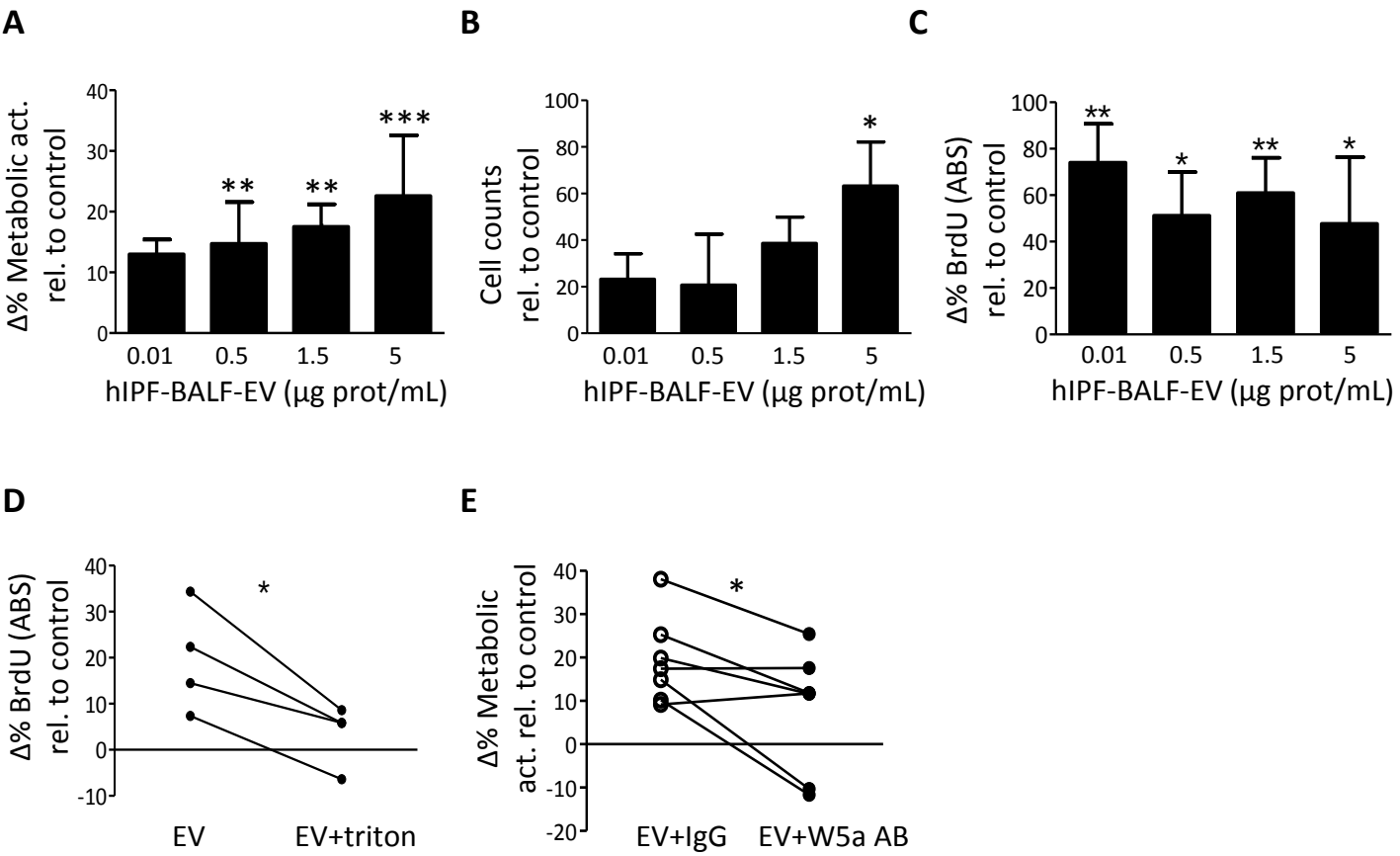

AJRCCM Articles in Press. Published on 25-July-2018 as 10.1164/rccm.201708-1580OC

Online Data Supplement

Increased extracellular vesicles mediate WNT-5A signaling in idiopathic pulmonary fibrosis

Supplemental materials and methods

Patient cohorts for bronchoalveolar lavage fluid (BALF) analysis

Bronchoscopy with bronchoalveolar lavage (BAL) was performed in a single sub-segment of the right middle lobe or lingual and BAL fluid (BALF) was collected according to a standardized protocol (1) with a total of 100 mL of sterile saline instilled, and similar returns among subject groups; analytes were normalized by volume. The BALF was kept on ice and processed within 1 hour of collection then frozen at –80C. BALF was collected in two independent cohorts (Munich and UCSF, respectively). All patient diagnoses were made in accordance with established criteria (2). In case of Non-ILD patients, BALF was performed for diagnostic evaluation (unclear cough) and ILD was excluded (see also Table 1). The diagnosis of non-IPF ILD and IPF was determined by a pathology core consisting of two pulmonary pathologists, a radiology core consisting of three pulmonary radiologists, and a clinical core consisting of five pulmonary physicians. Informed consent was obtained from every patient in order to collect human BALF from both cohorts of patients. The Munich study was approved by the ethics committee at the LMU (Ludwig-Maximilians Universität München, Germany, Ethics Approval 382-10) and patient characteristics are presented in Table 1. The UCSF study cohort was approved by the University of California San Francisco (UCSF) ethics committee (study #12-09662) and patient characteristics are presented in Table 2.

Patient cohorts for lung tissue homogenates and cell isolations

All lung tissue samples were collected in frame of the European IPF registry (eurIPFreg) and provided by either the UGMLC Giessen Biobank (member of the DZL Platform Biobanking, Ethics Approval No. 111/08

and 58/15) or the CPC Bioarchive CPC-M at the University Hospital Grosshadern of the Ludwig Maximilian University (Ethics Approval 333-10, 455-12). Control tissue was obtained from transplant specimens that failed lung transplantation criteria. Lung tissue homogenates from 6 patients with sporadic IPF (mean age (years): 51 (42-61) and 6 non-disease controls (organ donors; mean age (years): 54 (42-62) were used for Western Blot analysis in Figure 2C. Lung tissue homogenates from 7 patients with sporadic IPF (mean age (years)): 49 (34-61) and 7 non-disease controls (organ donors; mean age (years): 54 (42-61) were used for Western Blot analysis in Figure 2F. The phATII cells were isolated as previously described (3, 4) and the isolation of phLFs was also performed as previously described (5).

Cell culture

The phATII cells were cultured in Dulbecco's Modified Eagle's medium/Nutrient mixture F12 medium (DMEM/F-12) supplemented with 10% (v/v) FCS (Pan-Biotech, Germany), and 1% (v/v) antibiotics (100 µg/ml streptomycin and 100 U/ml penicillin, Gibco, USA). 48h post-isolation, cells were washed with PBS and cultured for 48h in DMEM/F-12 supplemented with 1% of extracellular vesicle (EV)-depleted FCS (System Biosciences, USA) and 1% (v/v) antibiotics. The phLFs were grown to 80% confluence in DMEM/F-12 supplemented with 20% (v/v) FCS, and 1% (v/v) antibiotics (100 µg/ml streptomycin and 100 U/ml penicillin). Cells were then starved in 0.1% FCS 1% antibiotics medium for 24 h and, afterwards, all treatments were performed for 48 h in EV-depleted medium; DMEM/F-12 supplemented with 1% EV-depleted-FCS (System Bioscience, USA), and 1% antibiotics. The phLFs were treated with TGFβ (2ng/ml) or BSA as control prior to EV isolation. 50ml of the supernatants from each condition were used for EV isolation. Depletion of WNT ligand secretion was performed by treatment of phLFs with 100nM of IWP2 (Sigma Aldrich) or DMSO as vehicle (treatments were refreshed once after 24 h by adding IWP2 or DMSO to the supernatants). 1ml of the supernatants was collected to confirm WNT-5A depletion, and the remaining volume was subjected to EV isolation.

AJRCCM Articles in Press. Published on 25-July-2018 as 10.1164/rccm.201708-1580OC

Animals

Female C57BL/6N mice free of pathogen of 8-10 week-old (Charles River Laboratories, Sulzfeld, Germany) were used for experimental lung fibrosis. All animal studies were conducted under strict governmental and international guidelines and approved by the local government for the administrative region of Upper Bavaria (Project 55.2-1-54-2532-88-12). To induce lung fibrosis, mice were instilled intratracheally with 2U of Bleomycin (Almirall, Barcelona, Spain) per kg body weight dissolved in 50 µl of sterile PBS applied as a single dose per animal using the Micro-Sprayer Aerosolizer, Model IA-1C (Penn-Century, Wyndmoor, PA). PBS alone was instilled as control. At day 14 post-instillation, mice were sacrificed for the extraction of BALF and lung lobes. The 3D-Lung Tissue Cultures were generated from bleomycin- or PBS-treated mice (day 14 post-instillation) as described in (6) and kept in culture for 72 hours in EV-depleted medium supplemented with 2.5% amphotericin B (Sigma Aldrich, St Louis, MO) for subsequent EVs isolation.

WNT-5A inhibition

For WNT-5A neutralizing antibody experiments, EV-Pellets from phLFs were incubated with 1µg of either αWNT-5A antibody (RND systems: MAB645) or control IgG antibody (RND systems: MAB006) for 30 min before stimulation. For WNT-5A siRNA experiments, phLFs were transfected as described before (5). To analyze Cyclin-D1 expression, cells were further starved in 0.1% FCS, 1% antibiotics DMEM/F-12 medium for 24 h. For the other analysis, cells were kept in EV-depleted medium for 48 h prior to the isolation of EVs that were used for functional experiments.

Proliferation assay

Protein content was quantified by Pierce™ BCA Protein Assay Kit (Thermofisher Scientific, Massachusetts USA) in EV-Pellets obtained from the treatments in phLFs mentioned above or from BALF from IPF

patients. Next, EV-Pellets were used at concentrations of 0.01, 0.5 or 1.5 µg protein/ml to treat donor phLFs (previously seeded in a 96-well plate at density of 5.000 cells/well) for 48 h. Proliferation was assessed by cell counting, WST-1 Cell Proliferation Reagent (ab155902, Abcam, Cambridge, UK) and BrdU cell proliferation kit (#6813, Cell Signaling, USA) according to manufacturer's instructions.

Immunoblotting

Cells, lung homogenates and EV-Pellets were lysed in Radio-Immunoprecipitation Assay (RIPA) buffer supplemented with protease and phosphatase inhibitors (Roche Diagnostics, Mannheim, Germany) and protein concentrations were quantified using a BCA assay (Bio-Rad). Samples were concentrated if necessary by Amicon Ultra-0.5 centrifugal filters (Merck Millipore, Amsterdam, The Netherlands). Reducing conditions (4x Laemmli loading buffer: 150 mM Tris HCl, 275 mM SDS, 400 mM dithiothreitol, 3.5% (w/v) glycerol, 0.02% bromophenol blue) were used for the detection of GPR177 and non-reducing (without dithiothreitol) for the rest of proteins. For murine BALF-EVs, whole EV-Pellets lysates were loaded into the gel, whereas a constant protein amount (10 µg) was used for comparison of EVs obtained from 3D-LTCs, human BALF and phLFs or phATII cell culture supernatants. Samples were loaded into a 10% SDS-PAGE gel and transferred to a nitrocellulose membrane that was blocked afterwards in 1x RotiBlock (Carl Roth, Germany). Blocked membranes were incubated with primary antibodies directed against TGS101 (HPA006161, Sigma Aldrich), CD81 (DLN-09707, Dianova, Hamburg, Germany), Calreticulin (#2891S, Cell Signaling, USA), GPR177 (sc-13635, Santa Cruz Biotechnology, CA, USA) or WNT-5A (MAB645, R&D systems, Abingdon, UK) at dilution of 1:1000 in 1x RotiBlock. Finally, membranes were incubated with HRP-conjugated secondary antibodies anti-rabbit (NA934V) and anti-rat (NA935V) from GE healthcare (Munich, Germany). The signal was detected by enhanced chemiluminescence reagents (Pierce ECL, Thermo Scientific, Ulm, Germany) and it was imaged at ChemiDoc™ XRS+ system

AJRCCM Articles in Press. Published on 25-July-2018 as 10.1164/rccm.201708-1580OC

(Biorad, Munich, Germany). Ponceau S staining (Sigma Aldrich) or HRP-conjugated β-actin (A3854, Sigma Aldrich) were used as loading controls.

Quantitative RT-PCR

Total RNA was isolated from cells or lung homogenates using the RNeasy Mini Kit (Qiagen, Hilden, Germany) according to the manufacturer's instructions. Reverse transcription was performed by SuperScriptII (Life Technologies) and cDNA products were subjected to quantitative RT-PCR using SYBR Green and LightCycler 480 system (Roche). Mouse and human Hypoxanthine-guanine phosphoribosyltransferase (*Hprt*) was used as housekeeping gene for all the experiments. The following primers were used for the reactions: human *WNT-5A* 5´CCAAGGGCTCCTACGAGAGTGC3´, 3´CACATCAGCCAGGTTGTACACCG5´; human *CCND1* 5´CCGAGAAGCTGTGCATCTACAC3´, 5´AGGTTCCACTTGAGCTTGTTCAC3´; human *FN1* 5´GGATGTGTGGCAGATAGGATGTATT3´, 3´CAATGCGGTACATGACCCCT5´; human *ACTA2* 5´CGAGATCTCACTGACTACCTCATGA3´, 3´AGAGCTACATAACACAGTTTCTCCTTGA5´; human *COL1A1* 5'CAAGAGGAAGGCCAAGTCGAG'3, 5'TTGTCGCAGACGCAGATCC'3; human *TNC* 5´CCATCTATGGGGTGATCCGG3´, 3´TCGGTAGCCATCCAGGAGAG5´, and mouse *Wnt-5a* 5´GACTCCGCAGCCCTGCTTTG3´, 5´CCAATGGGCTTCTTCATGGCGAG3´.

Nanoparticle tracking analysis

Quantification and size distribution assessment of EV following isolation were analyzed using a particle-tracking system (NanoSight NS300, Malvern Panalytical, UK). In brief, diluted EV samples (in 500µl of PBS) were injected at a constant flow into the fluidic chip using a single syringe pump module. Vesicle courses were recorded with a fast video capture system for a total of 5 records of 30 sec each. Based on the dynamic light scattering and the Brownian motion of individual vesicles, the dedicated software (NTA 3.1, Malvern Panalytical, UK) reported a profile of the EV preparation with both vesicle size and

concentration. For quantification of EV, concentration of EVs has been calculated from 3 (for mouse BALF) or 5 (for human BALF) replicate measurements according to the sample volumes and expressed as number of EVs per ml of initial sample.

Transmission electron microscopy

To characterize the morphology of the vesicles by transmission electron microscopy, EVs were serial diluted and collected in carbon-coated copper grids, then the samples were stained with uranyl acetate and imaged using a Zeiss Libra 120 Plus microscope (Carl Zeiss NTS GmbH).

Disruption of EV membrane by detergent

EV-Pellets from phLFs or BALF from IPF patients were incubated with 0.075% triton (diluted in 0.1% EV-depleted FCS containing medium) for 30 minutes as previously described (7) and then used to treat donor phLFs at the concentration of 0.5µg EV prot./mL for the functional analysis. EV-free medium at the same concentration of triton without EVs was used as control.

Statistical analysis

All data is expressed as mean±SD and analyzed with GraphPad Prism 5 software (La Jolla, CA, USA). Student's *t* test was used with comparison between PBS and bleomycin groups, whereas paired Student's *t* test was applied to experiments involving phLFs. For comparison of more than 2 groups, One-way ANOVA was used followed by Dunnett´s or Bonferroni post-hoc test. Normal distribution of the data distribution was determined by Kolmogorov-Smirnov testing with Lilliefors' correction before applying unpaired Student's *t* test.

AJRCCM Articles in Press. Published on 25-July-2018 as 10.1164/rccm.201708-1580OC

Supplementary Figure Legends

Supplementary figure E1: Characterization of EVs isolated in mouse and human BALF. (A) Representative images of transmission electron microscopy, and (B) protein analysis of the EV-marker TSG101 in EV-free-supernatants (EV-free-SN) and EV-Pellets (EV-P) of BALF from PBS- or bleomycin-treated mice. (C) Analysis of the size distribution of EVs by dynamic light scattering in BALF-EVs from PBS- (left) and bleomycin-treated mice (right). EV-Pellets were serial diluted to fit the range of sensitivity. EVs were isolated by ExoQuick®. Pool of 2 mouse BALFs per n; n=3 per group. (D) Protein analysis of the ER-marker Calreticulin and the EV-enriched protein TSG101 in cell lysates (CL), pure BALF (pBALF), EV-Pellets (EV-P) and EV-free-BALF-supernatants (EV-free-SN) of human BALF sample from patients with non-IPF ILD, IPF or non-ILD. EVs were isolated by ultracentrifugation. Ponceau S staining was used as loading confirmation.

Supplementary figure E2: EV are dysregulated during IPF. (A) Correlation of lung function parameter (%FVC) with EV amount isolated from BALF of patients with IPF (UCSF Cohort, Fig 1H). Dots represent single patient values, correlation coefficient is indicated. (B) Comparison of EV amount secreted in BALF from non-IPF and IPF patients. Quantification by nanoparticle tracking analysis of EV amount in BALF from non-IPF (n=21) and IPF (n=13) patients. The data of 2 different cohorts was combined (white; Munich cohort, grey; UCSF cohort). Measurements were done in 5 replicates. Unpaired Student's *t* test, *P<0.05.

Supplementary figure E3: Correlation of WNT-5A with TSG101 expression in EVs isolated from human BALF. Graph representing the band intensity of WNT5A and TSG101 from Fig. 3D (dots represent single values; linear regression test; P<0.05).

Supplementary figure E4: Characterization of EVs isolated from cell culture supernatants. Nanoparticle tracking analysis (mean±SD; 5 measurements performed each) of EVs isolated from primary human lung fibroblasts.

Supplementary figure E5: Effect of primary human lung fibroblasts-derived EVs on (myo)fibroblast gene expression. phLFs were treated with EVs derived from the same patient at the concentration of 1.5µg EV prot/mL (n=6-9) and mRNA levels of *FN1*, *ACTA2, COL1A1* and *TNC* were assessed. Paired Student's *t* test; *P<0.05, **P<0.01.

Supplementary figure E6: Characterization of EVs upon WNT-5A silencing in primary human lung fibroblast. (A) Protein analysis of the EV-enriched proteins TSG101 and CD81 in EV-Pellets isolated from phLF transfected with a siRNA targeting WNT-5A or a control siRNA (left panel). Ponceau S staining was used as loading confirmation and to normalize protein expression. Densitometry of CD81 (middle) and TSG101 (right) relative to Ponceau are presented. (B) Quantification by nanoparticle tracking analysis of EV secretion from phLF transfected with a siRNA targeting WNT-5A or a control siRNA. Paired Student's *t* test.

AJRCCM Articles in Press. Published on 25-July-2018 as 10.1164/rccm.201708-1580OC

Uncategorized References

1. Goldstein RA, Rohatgi PK, Bergofsky EH, Block ER, Daniele RP, Dantzker DR, Davis GS, Hunninghake GW, King TE, Jr., Metzger WJ, et al. Clinical role of bronchoalveolar lavage in adults with pulmonary disease. *Am Rev Respir Dis* 1990; 142: 481-486.
2. Raghu G, Collard HR, Egan JJ, Martinez FJ, Behr J, Brown KK, Colby TV, Cordier JF, Flaherty KR, Lasky JA, Lynch DA, Ryu JH, Swigris JJ, Wells AU, Ancochea J, Bouros D, Carvalho C, Costabel U, Ebina M, Hansell DM, Johkoh T, Kim DS, King TE, Jr., Kondoh Y, Myers J, Muller NL, Nicholson AG, Richeldi L, Selman M, Dudden RF, Griss BS, Protzko SL, Schunemann HJ, Fibrosis AEJACoIP. An official ATS/ERS/JRS/ALAT statement: idiopathic pulmonary fibrosis: evidence-based guidelines for diagnosis and management. *American journal of respiratory and critical care medicine* 2011; 183: 788-824.
3. Konigshoff M, Kramer M, Balsara N, Wilhelm J, Amarie OV, Jahn A, Rose F, Fink L, Seeger W, Schaefer L, Gunther A, Eickelberg O. WNT1-inducible signaling protein-1 mediates pulmonary fibrosis in mice and is upregulated in humans with idiopathic pulmonary fibrosis. *J Clin Invest* 2009; 119: 772-787.
4. Mutze K, Vierkotten S, Milosevic J, Eickelberg O, Konigshoff M. Enolase 1 (ENO1) and protein disulfide-isomerase associated 3 (PDIA3) regulate Wnt/beta-catenin-driven trans-differentiation of murine alveolar epithelial cells. *Dis Model Mech* 2015; 8: 877-890.
5. Baarsma HA, Skronska-Wasek W, Mutze K, Ciolek F, Wagner DE, John-Schuster G, Heinzelmann K, Gunther A, Bracke KR, Dagouassat M, Boczkowski J, Brusselle GG, Smits R, Eickelberg O, Yildirim AO, Konigshoff M. Noncanonical WNT-5A signaling impairs endogenous lung repair in COPD. *J Exp Med* 2017; 214: 143-163.
6. Lehmann M, Korfei M, Mutze K, Klee S, Skronska-Wasek W, Alsafadi HN, Ota C, Costa R, Schiller HB, Lindner M, Wagner DE, Gunther A, Konigshoff M. Senolytic drugs target alveolar epithelial cell function and attenuate experimental lung fibrosis ex vivo. *Eur Respir J* 2017; 50.
7. Osteikoetxea X, Sodar B, Nemeth A, Szabo-Taylor K, Paloczi K, Vukman KV, Tamasi V, Balogh A, Kittel A, Pallinger E, Buzas EI. Differential detergent sensitivity of extracellular vesicle subpopulations. *Organic & biomolecular chemistry* 2015; 13: 9775-9782.

Supplement figure E1

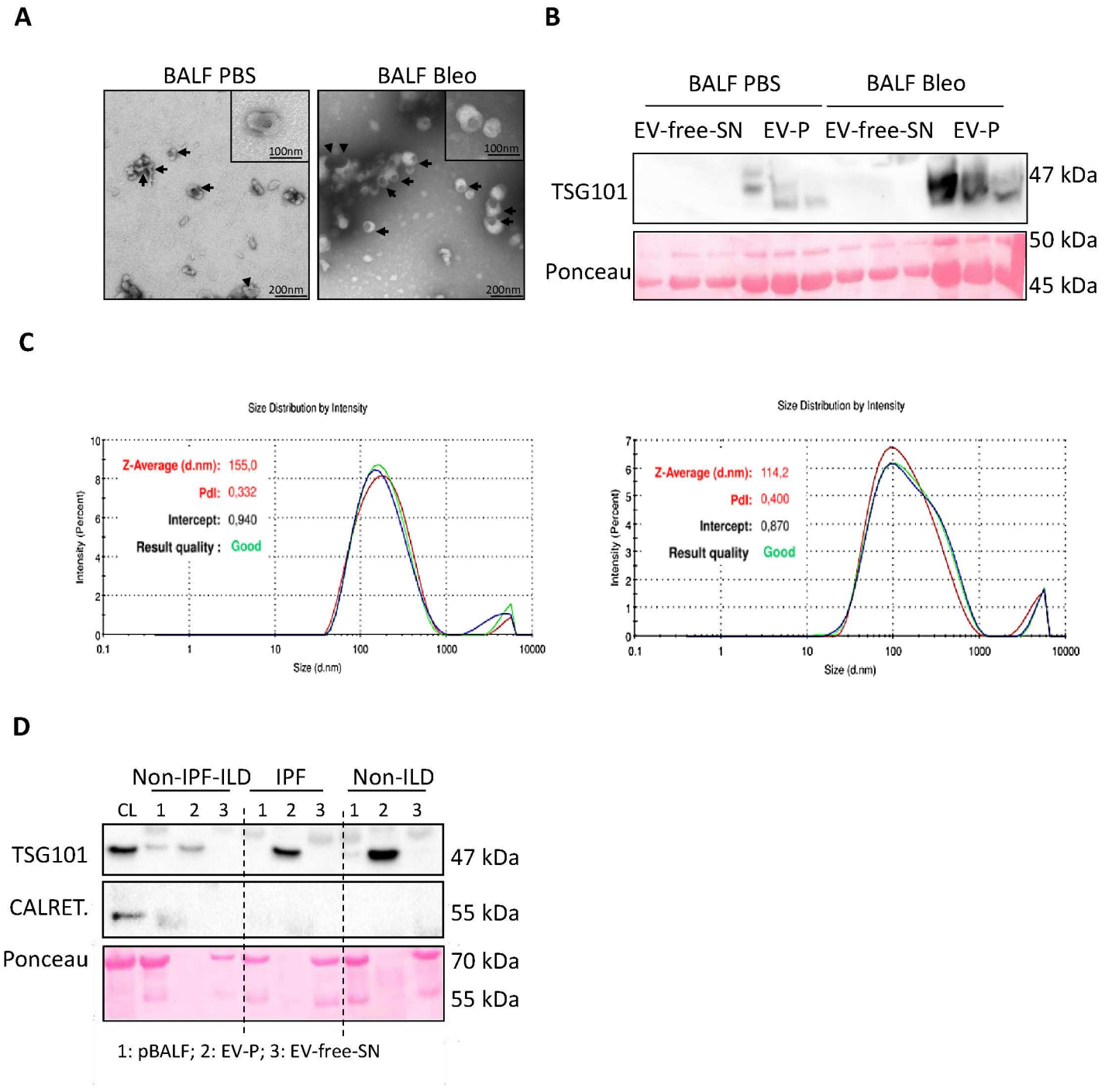

AJRCCM Articles in Press. Published on 25-July-2018 as 10.1164/rccm.201708-1580OC

Supplement figure E2

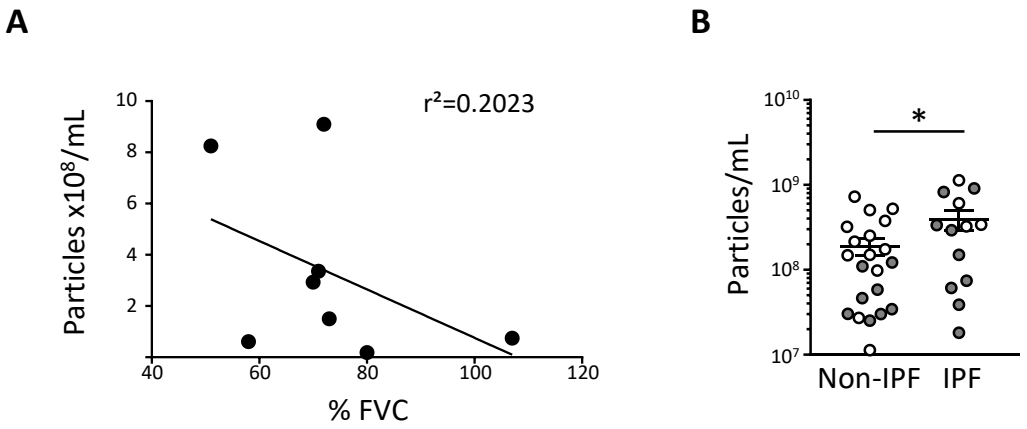

Supplement figure E3

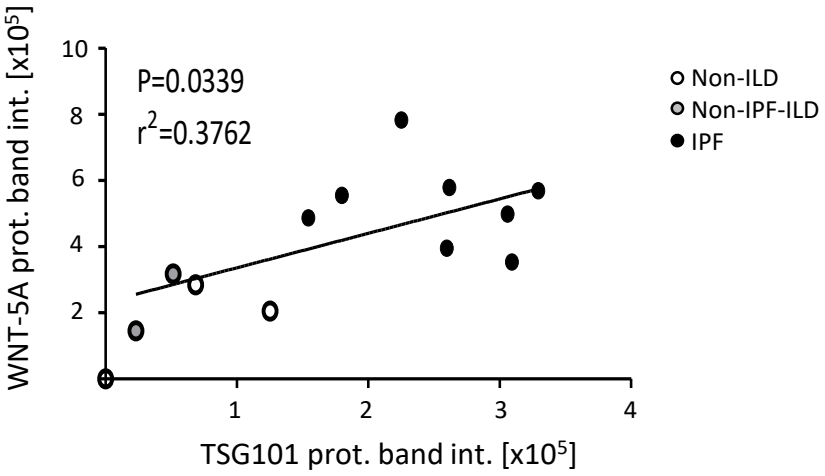

AJRCCM Articles in Press. Published on 25-July-2018 as 10.1164/rccm.201708-1580OC

Supplement figure E4

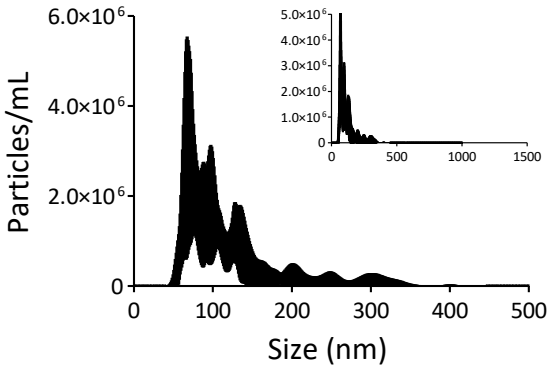

Supplement figure E5

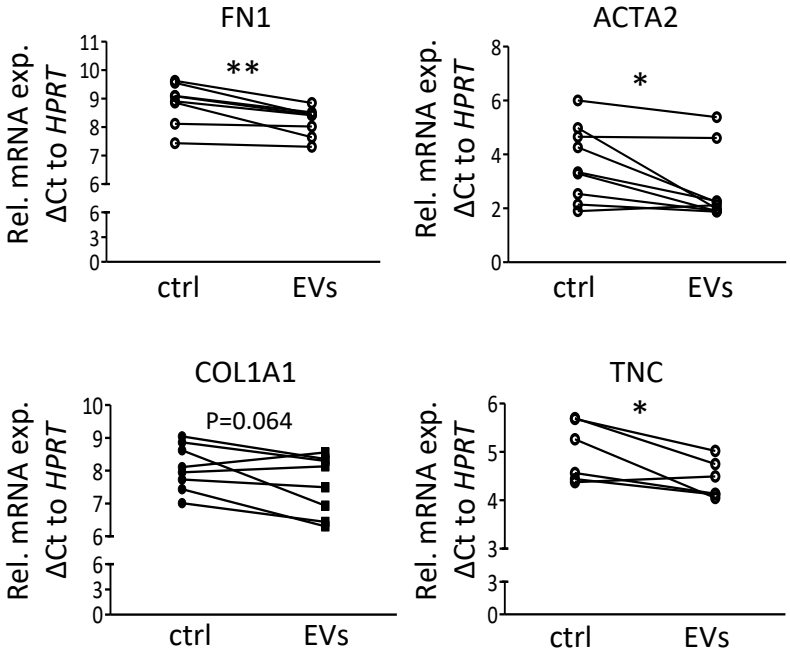

AJRCCM Articles in Press. Published on 25-July-2018 as 10.1164/rccm.201708-1580OC

Supplement figure E6